

# Semiconductor detectors - 3

Silvia Masciocchi,  
GSI and University of Heidelberg

*SS2017, Heidelberg  
June 14, 2017*

# Overview semiconductor detectors

- Principle of operation of semiconductor detectors
  - Properties of semiconductors (band structure)
  - Intrinsic material
  - Extrinsic (doped) semiconductors
  - p-n junction
- Signal generation
- Ionization yield and Fano factor
- Energy measurement with semiconductor detectors
- **Position measurement with semiconductor detectors**
  - **Micro-strip detectors: single- and double-sided, biasing schemes**
  - **Pixels: hybrid, monolithic active pixels, DEPFET**
  - **Silicon drift detectors**
  - **Charge-coupled devices (CCDs)**
  - **3D detectors**
- **Radiation damage**

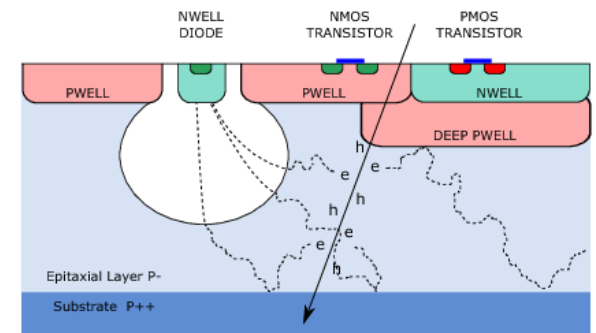
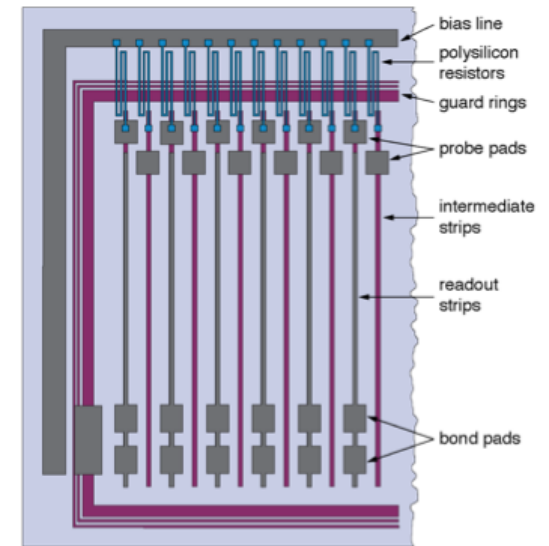
**May 24 and 31**

**TODAY**

# Position sensitive detectors

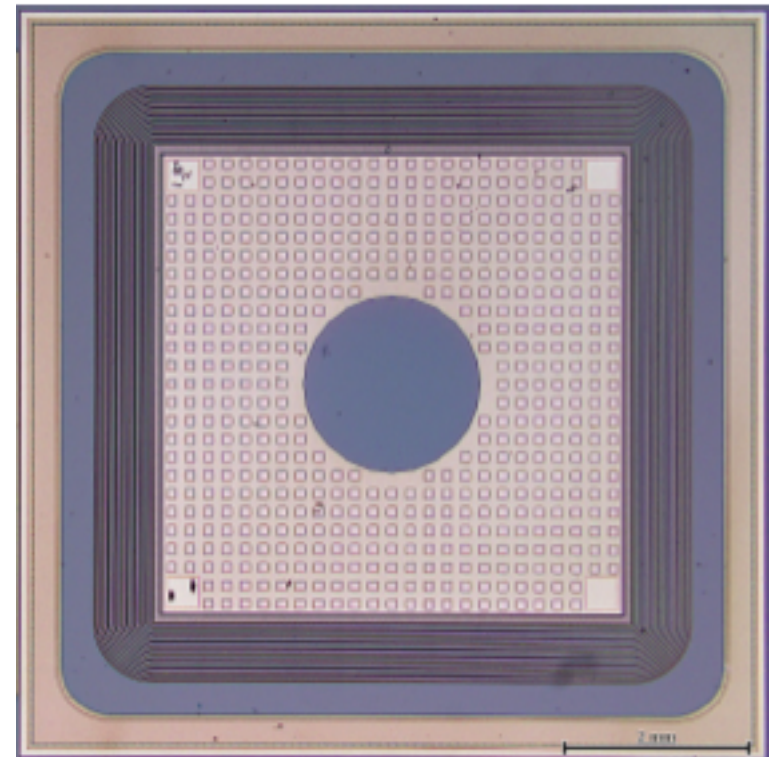
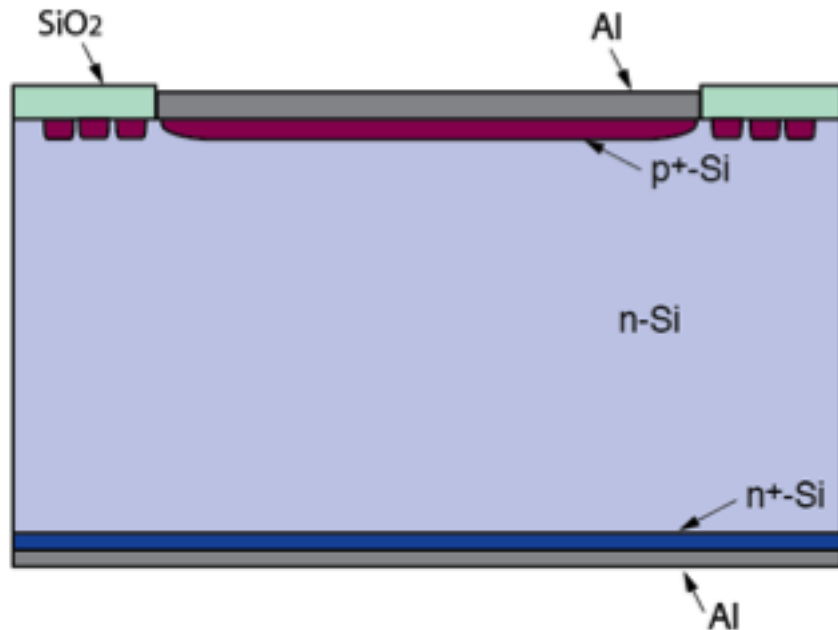
Detector structures:

1. Pad detector
2. Microstrip detectors: single sided  
DC coupled, AC coupled, biasing methods
3. Double-sided microstrip detectors
4. Hybrid pixel detectors
5. Silicon drift detectors
6. CCDs
7. Monolithic active pixel detectors
8. DEPFET detectors
9. 3D detectors
10. Avalanche photo diodes (APD)



# 1. Pad detector

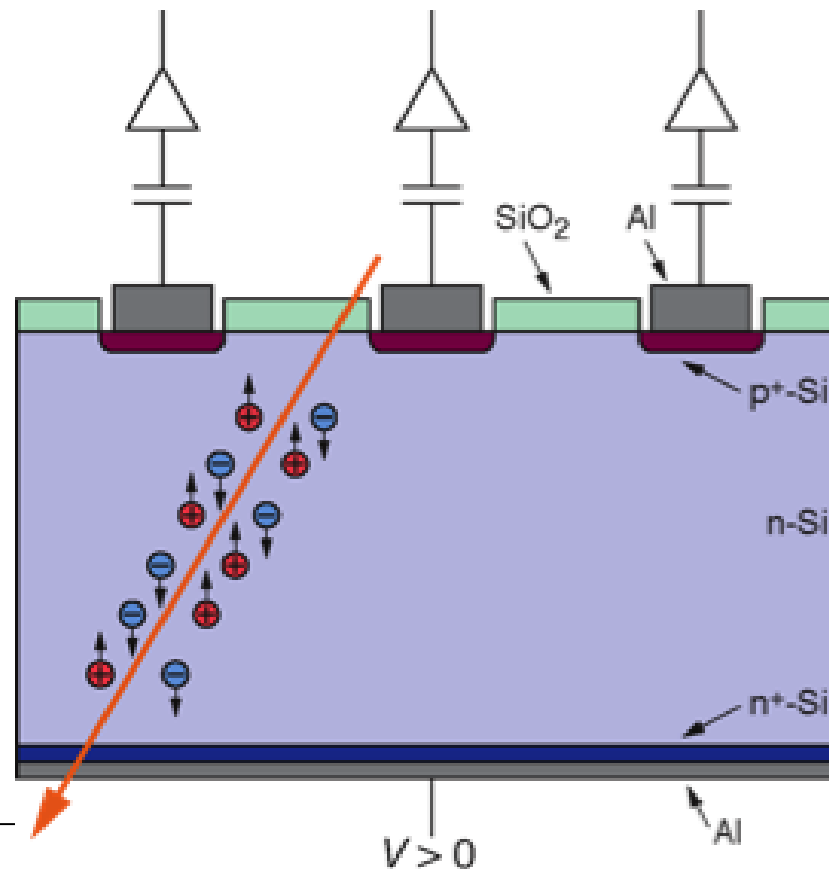
The most simple detector is a large surface **diode** with guard ring(s)



## 2. Microstrip detectors: DC coupling

Traversing charged particles create e-h<sup>+</sup> pairs in the depletion zone (about 30,000 pairs in standard detector thickness).

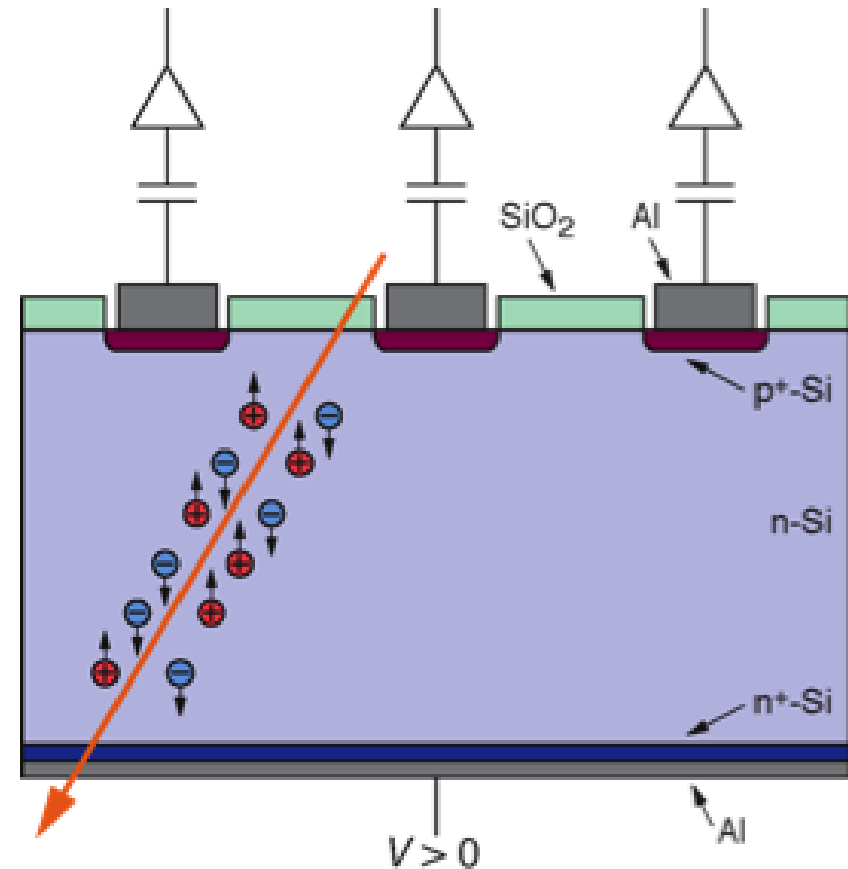
These charges drift to the electrodes. The drift (current) creates the signal which is amplified by an amplifier connected to each strip. From the signals on the individual strips the position of the traversing particle is deduced.



## 2. Microstrip detectors: DC coupling

A typical n-type Si strip detector:

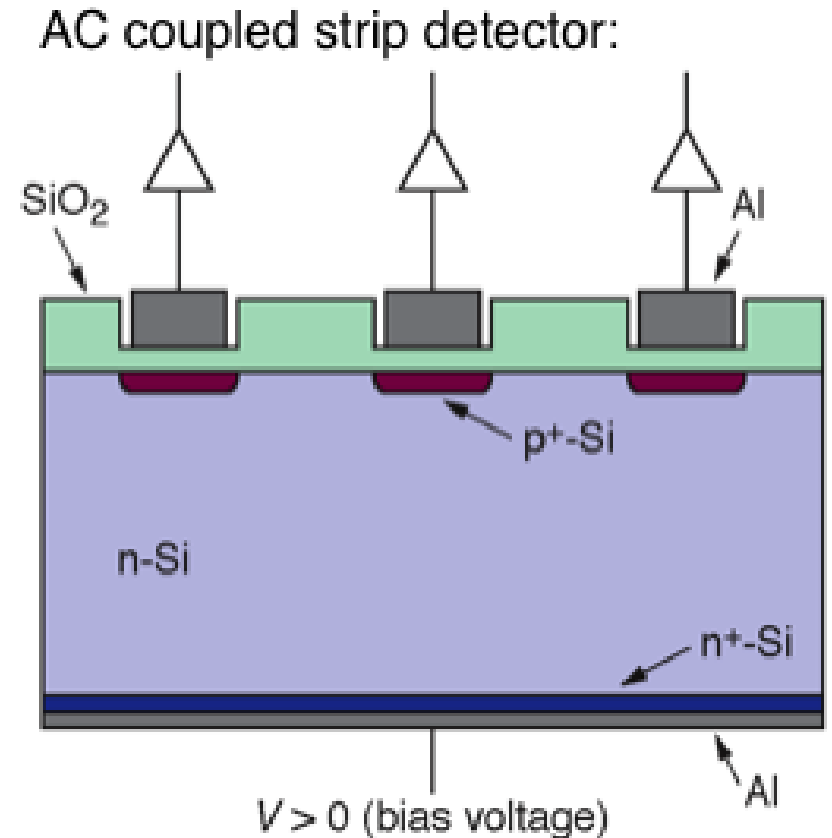
- p+n junction:  
 $N_a \approx 10^{15} \text{ cm}^{-3}$ ,  $N_d \approx 1\text{--}5 \cdot 10^{12} \text{ cm}^{-3}$
- n-type bulk:  $> 2 \text{ k}\Omega\text{cm}$
- thickness  $300 \text{ }\mu\text{m} \rightarrow 22,500 \text{ e-h pairs}$
- Operating voltage  $< 200 \text{ V}$
- n+ layer on backplane to improve ohmic contact
- Aluminum metallization
- Strip pitch  $25 - 100 \text{ }\mu\text{m}$
- Width of charge distribution  $\sim 10 \text{ }\mu\text{m}$
- Possible charge sharing by capacitive coupling ( $\sim 1 \text{ pF/cm}$ )



## 2. Microstrip detectors: AC coupling

AC coupling blocks leakage current from the amplifier:

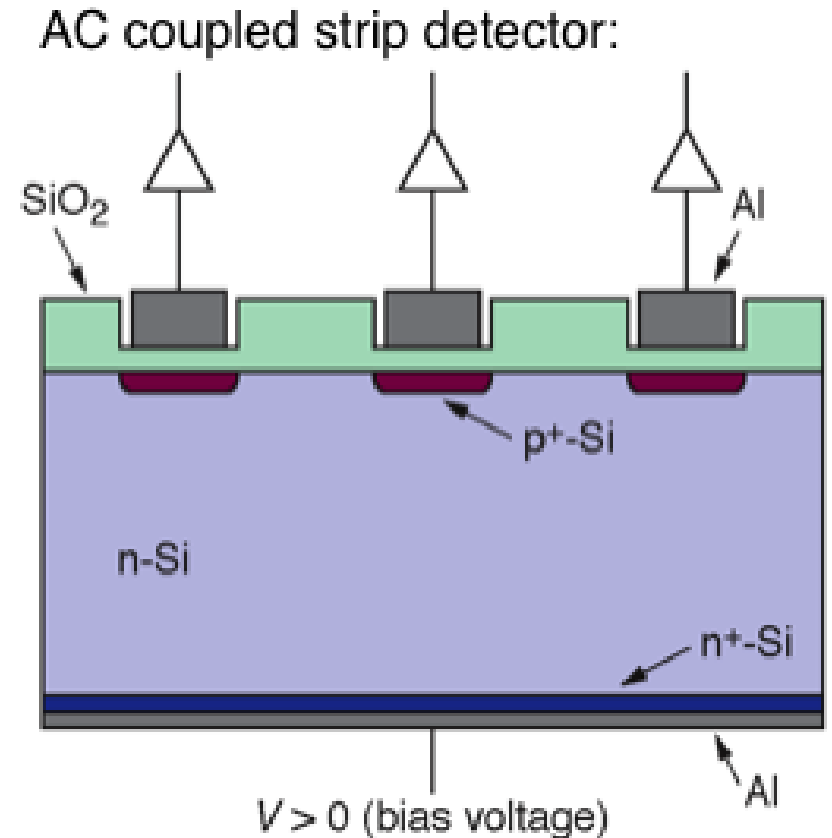
- Integration of coupling capacitances in standard planar process
- Deposition of  $\text{SiO}_2$  with a thickness of **100–200 nm** between p+ and aluminum strip
- Depending on oxide thickness and strip width the capacitances are in the range of 8–32 pF/cm
- Problems are shorts through the dielectric (pinholes). Usually avoided by a second layer of  $\text{Si}_3\text{N}_4$ .



## 2. Microstrip detectors: AC coupling

AC coupling blocks leakage current from the amplifier:

- Integration of coupling capacitances in standard planar process
- Deposition of  $\text{SiO}_2$  with a thickness of **100–200 nm** between p+ and aluminum strip
- Depending on oxide thickness and strip width the capacitances are in the range of 8–32 pF/cm
- Problems are shorts through the dielectric (pinholes). Usually avoided by a second layer of  $\text{Si}_3\text{N}_4$ .



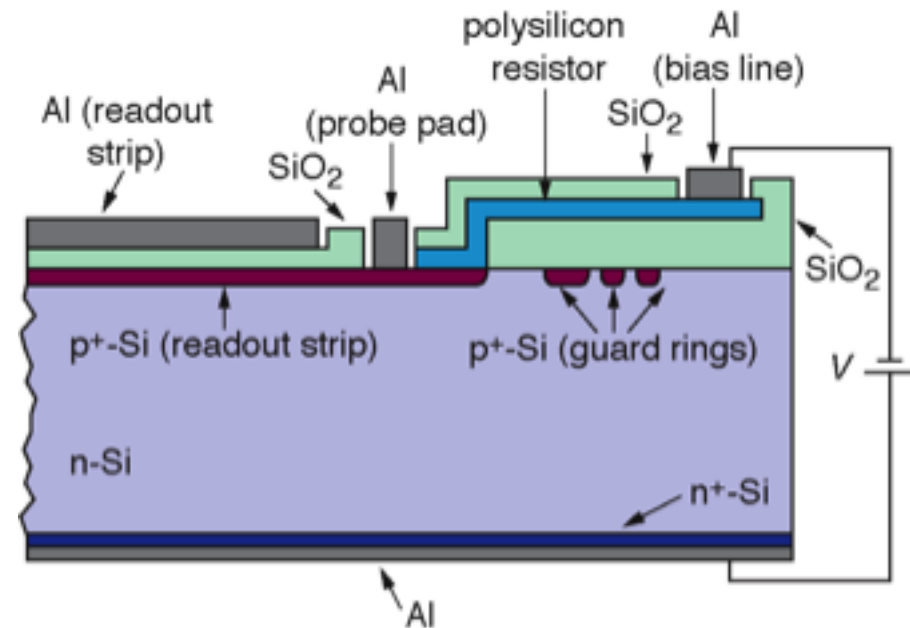
**However, the dielectric cuts the bias connection to the strips!**

Several methods to connect the bias voltage: polysilicon resistor, punch through bias, FOXFET bias.

## 2. AC-coupled microstrips: polysilicon resistors

- Deposition of polycrystalline silicon between p<sup>+</sup> implants and a common bias line
- Sheet resistance of up to  $R_s \approx 250 \text{ k}\Omega/\square$
- To achieve high resistor values winding poly structures are deposited. Depending on width and length a resistor of up to  $R \approx 20 \text{ M}\Omega$  is achieved ( $R = R_s \cdot \text{length}/\text{width}$ ).
- Drawback: Additional production steps and photo-lithographic masks required.

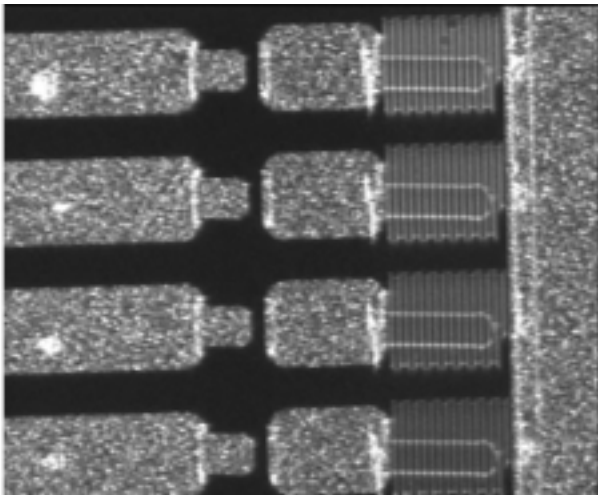
Cut through an AC coupled strip detector with integrated poly resistors



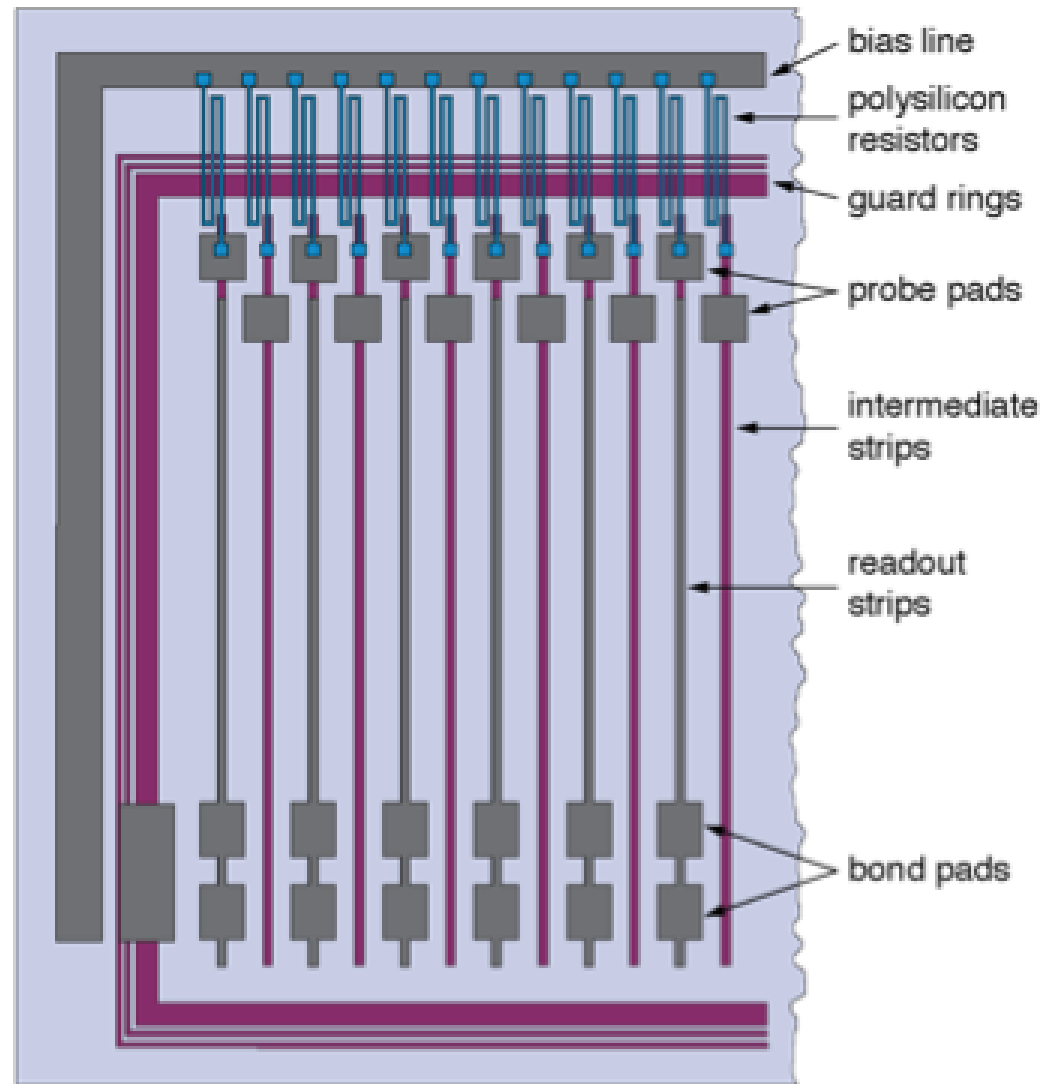
## 2. AC-coupled microstrips: polysilicon resistors

Top view of a strip detector with polysilicon resistors:

CMS-Microstrip-Detector: close view of area with polysilicon resistors, probe pads, strip ends.



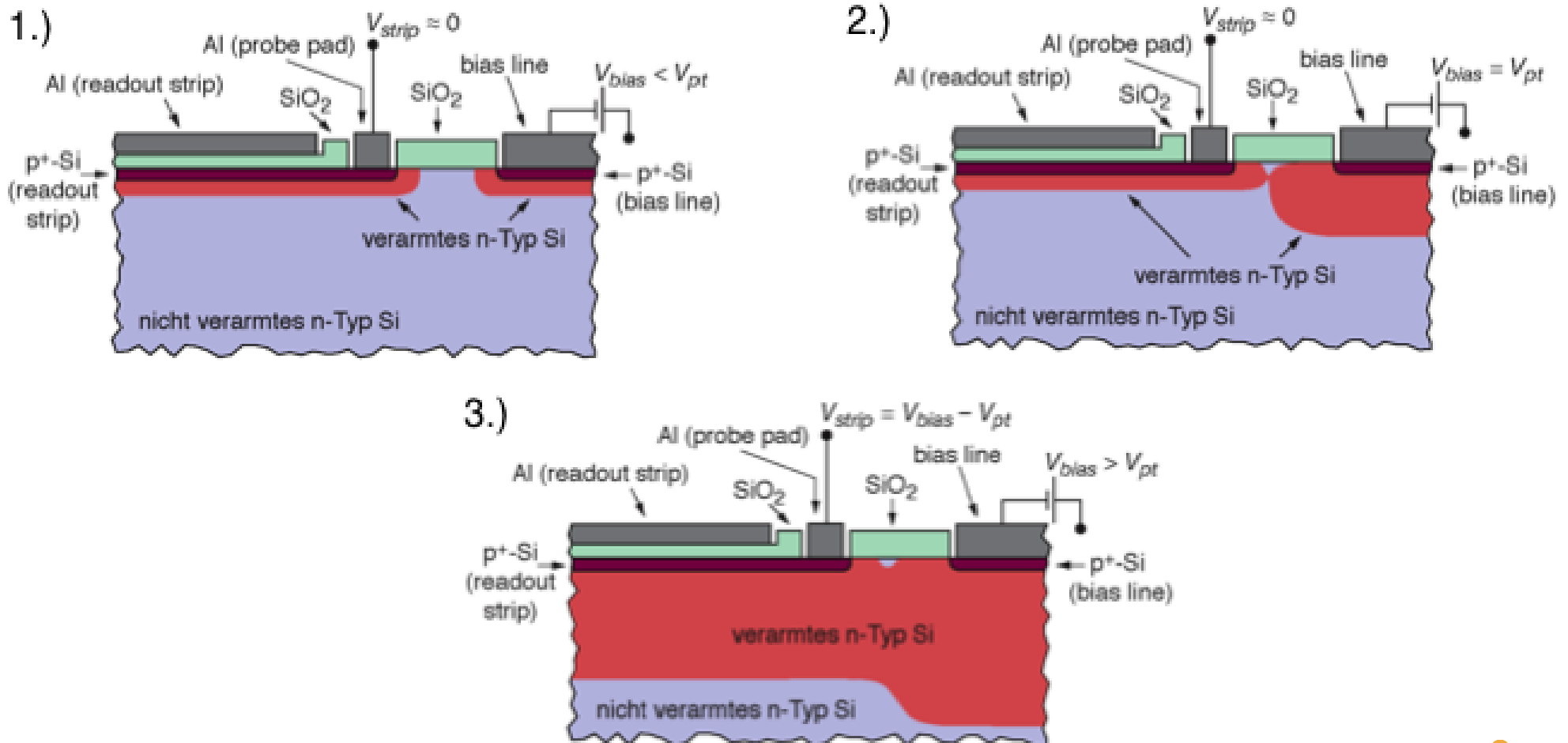
CMS Collaboration, HEPHY Vienna



## 2. AC-coupled microstrips: punch-through bias

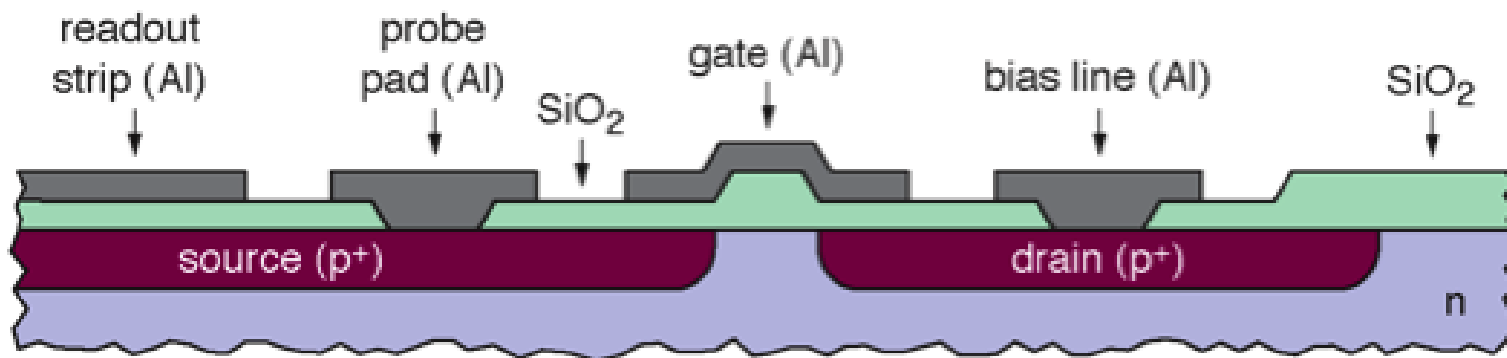
Punch through effect: figures show the increase of the depletion zone with increasing bias voltage ( $V_{pt}$  = punch through voltage).

Advantage: No additional production steps required.



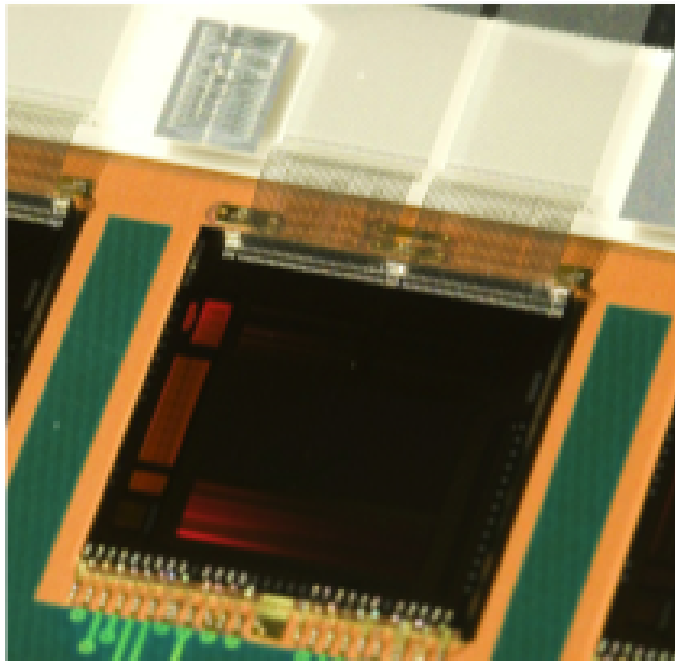
## 2. AC-coupled microstrips: FOXFET bias

- Strip p<sup>+</sup> implant and bias line p<sup>+</sup> implant are source and drain of a field effect transistor - FOXFET (**Field OXide Field Effect Transistor**).
- A gate is implemented on top of a SiO<sub>2</sub> isolation.
- Dynamic resistor between drain and source can be adjusted with gate voltage.



## 2. Microstrip: wire bond connection

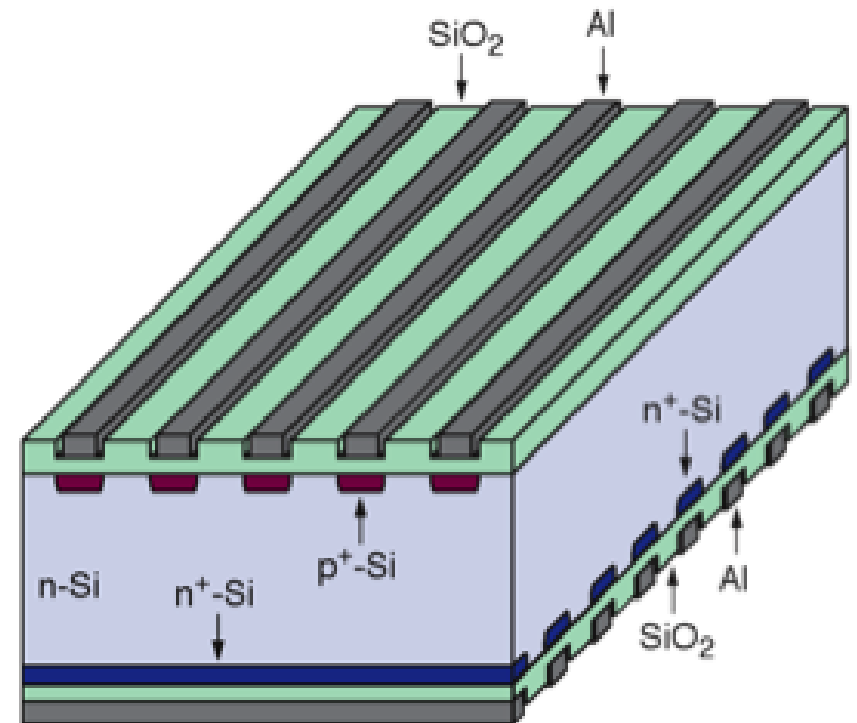
- Ultrasonic welding technique  
typically 25 micron bond wire of Al-Si-alloy
- Fully-automatized system with automatic pattern recognition



# 3. Double-sided microstrip detectors

- Single sided strip detector measures only one coordinate. To measure second coordinate requires second detector layer.
- Double sided strip detector measures two coordinates in one detector layer (minimizes material).
- In n-type detector the n<sup>+</sup> backside becomes segmented, e.g. strips orthogonal to p<sup>+</sup> strips.
- Drawback: Production, handling, tests are more complicated and hence double sided detector are expensive.

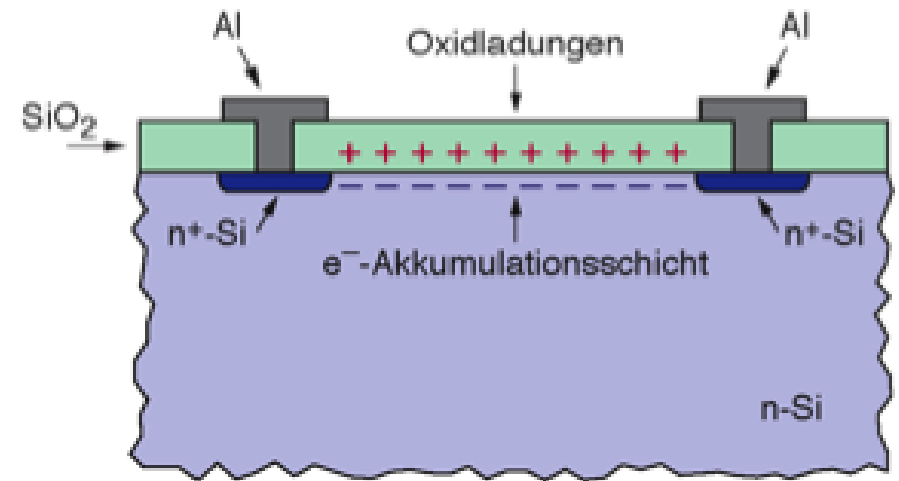
Scheme of a double sided strip detector (biasing structures not shown):



- Holes drift to p<sup>+</sup> strips
- Electrons drift to n<sup>+</sup> strips

# 3. Double-sided microstrip detectors

- Problem with n<sup>+</sup> segmentation: Static, positive oxide charges in the Si-SiO<sub>2</sub> interface.
  - These positive charges attract electrons. The electrons form an accumulation layer underneath the oxide.
  - n<sup>+</sup> strips are no longer isolated from each other (resistance ≈ kΩ)
  - Charges generated by through-going particle spread over many strips.
  - **No position measurement possible**
- Solution: Interrupt accumulation layer using p<sup>+</sup>-stops, p<sup>+</sup>-spray or field plates.

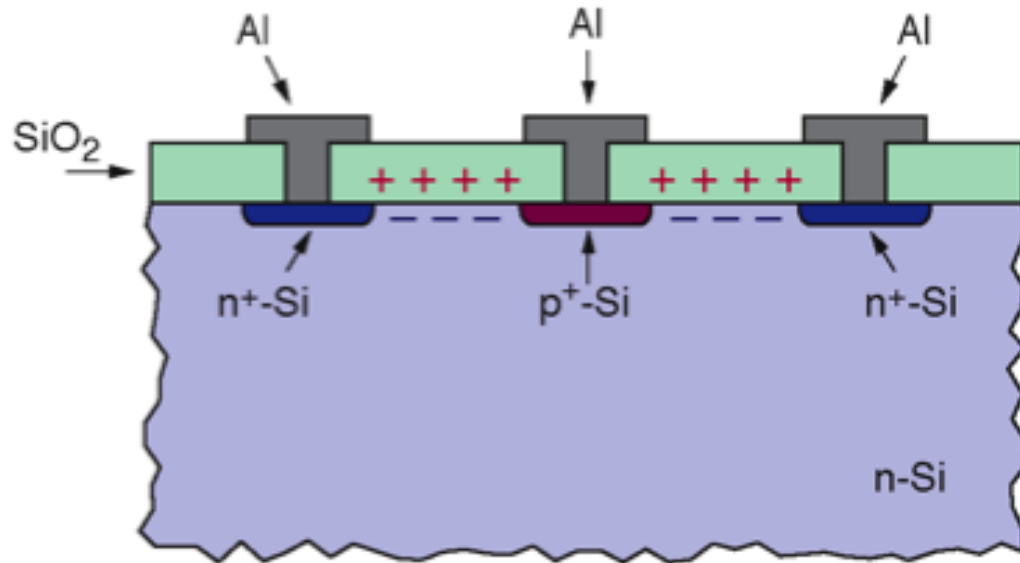


Positive oxide charges cause electron accumulation layer.

# 3. Double-sided: p<sup>+</sup>-stops

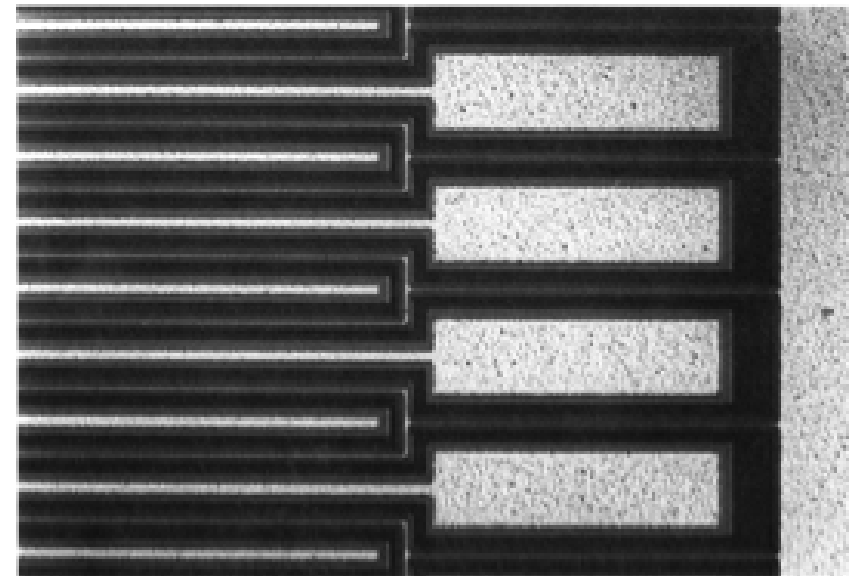
p<sup>+</sup>-implants (**p<sup>+</sup>-stops, blocking electrodes**) between n<sup>+</sup>-strips interrupt the electron accumulation layer.

→ Interstrip resistance reaches again G



A. Peisert, *Silicon Microstrip Detectors*, DELPHI 92-143 MVX 2, CERN, 1992

Picture showing the n<sup>+</sup>-strips and the p<sup>+</sup>-stop structure:

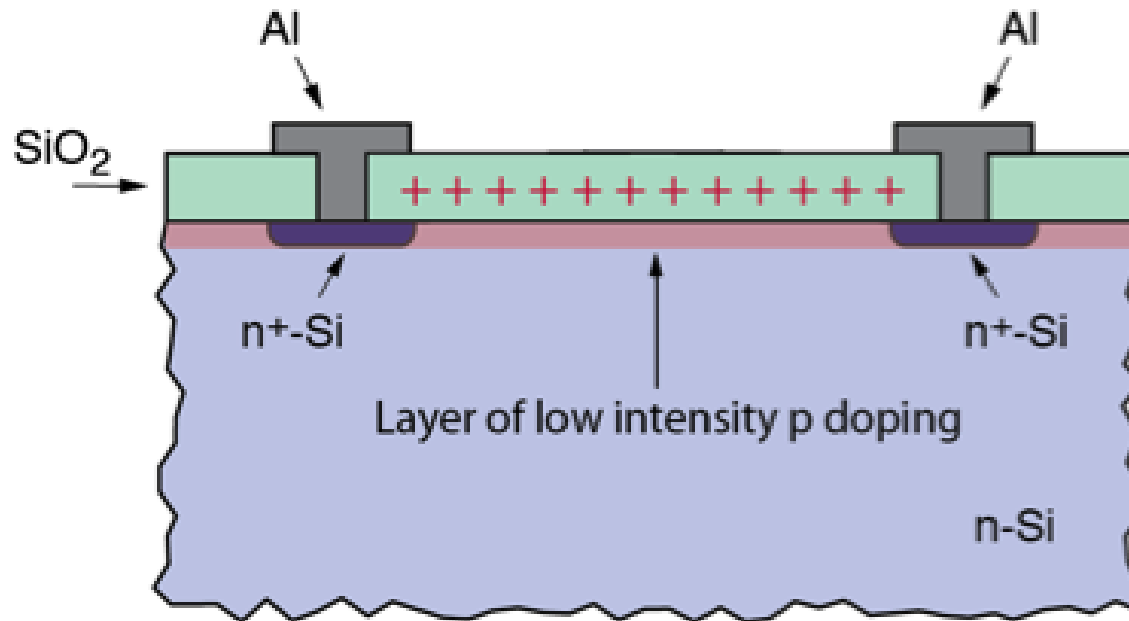


J. Kemmer and G. Lutz, *New Structures for Position Sensitive Semiconductor Detectors*, Nucl. Instr. Meth. A **273**, 588 (1988)

# 3. Double-sided: p-spray

p doping as a layer over the whole surface.

→ Disrupts the e- accumulation layer.



Some companies use a combination of p<sup>+</sup> stops and p spray

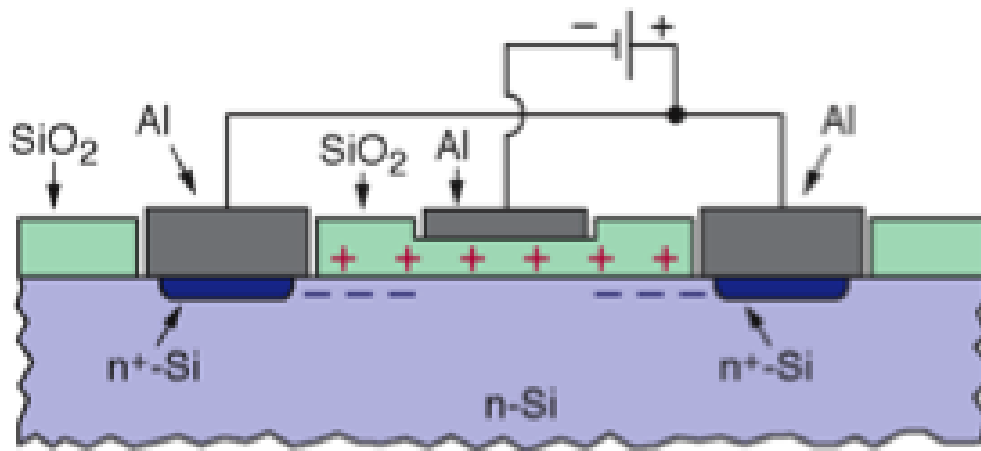
# 3. Double-sided: field plates

Metal of MOS structure at negative potential compared to the n<sup>+</sup>-strips displace electrons below Si-SiO<sub>2</sub>-interface.

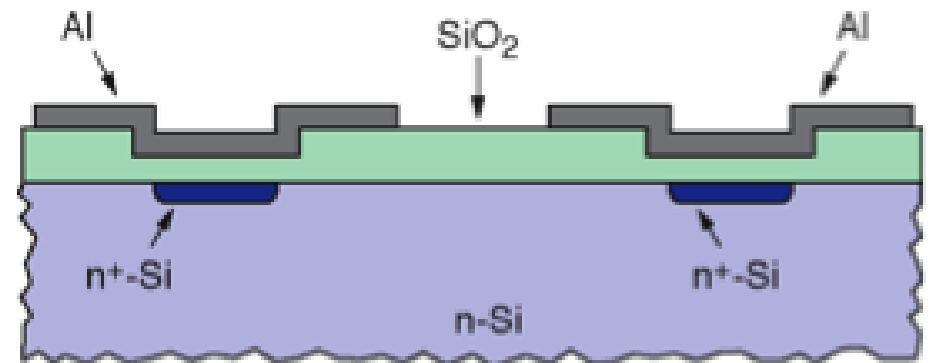
→ Above a threshold voltage n<sup>+</sup>-strips become isolated.

Simple realization of AC coupled sensors: Wide metal lines with overhang in the interstrip region serve as field plates.

A field plate at negative potential interrupts accumulation layer:



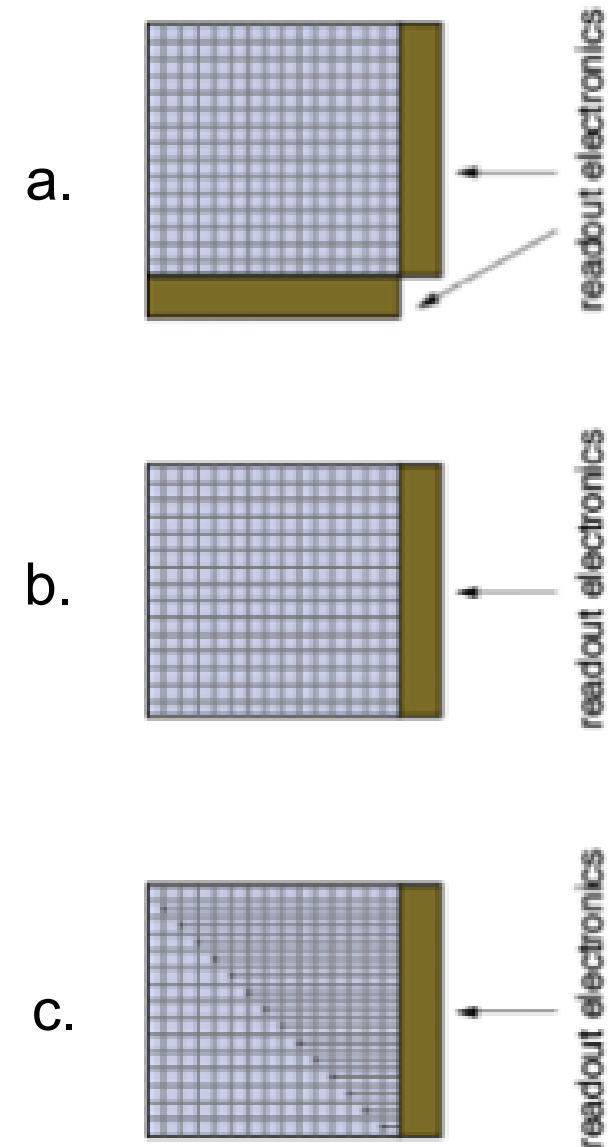
n<sup>+</sup>-strips of an AC coupled detector. The aluminum readout lines act as field plates:



A. Peisert, *Silicon Microstrip Detectors*, DELPHI 92-143 MVX 2, CERN, 1992

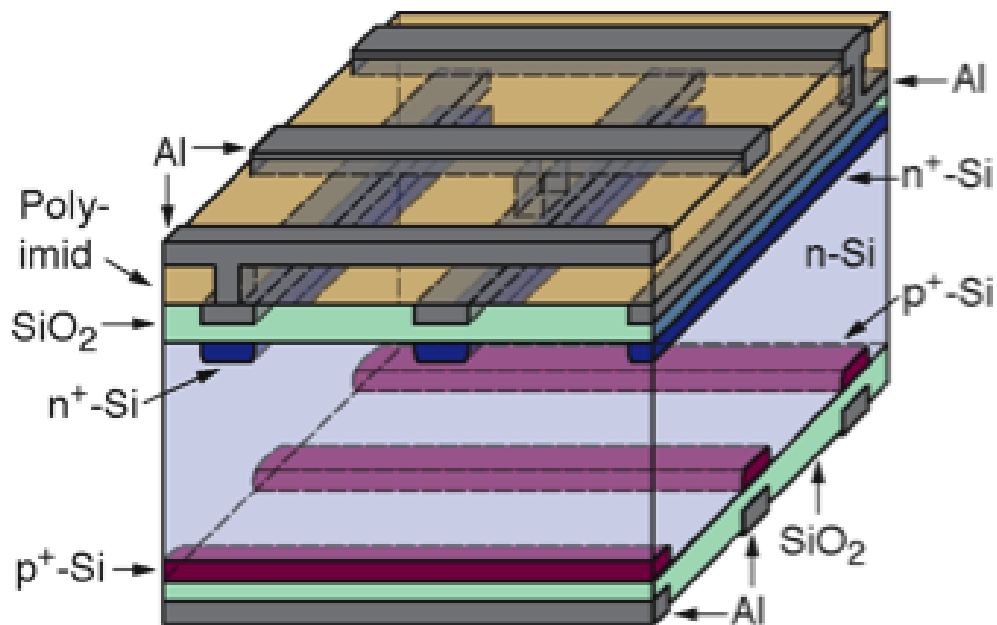
# 3. Double-sided double metal

- In the case of double sided strip detectors with orthogonal strips the readout electronics is located on two sides (fig. a).
- Many drawbacks for construction and material distribution, especially in collider experiments.
- Electronics only on one side is a preferred configuration (fig. b).
- Possible by introducing a **second metal layer**. Lines in this layer are orthogonal to strips and connect each strips with the electronics (fig. c). The second metal layer can be realized by an external printed circuit board, or better integrated into the detector.

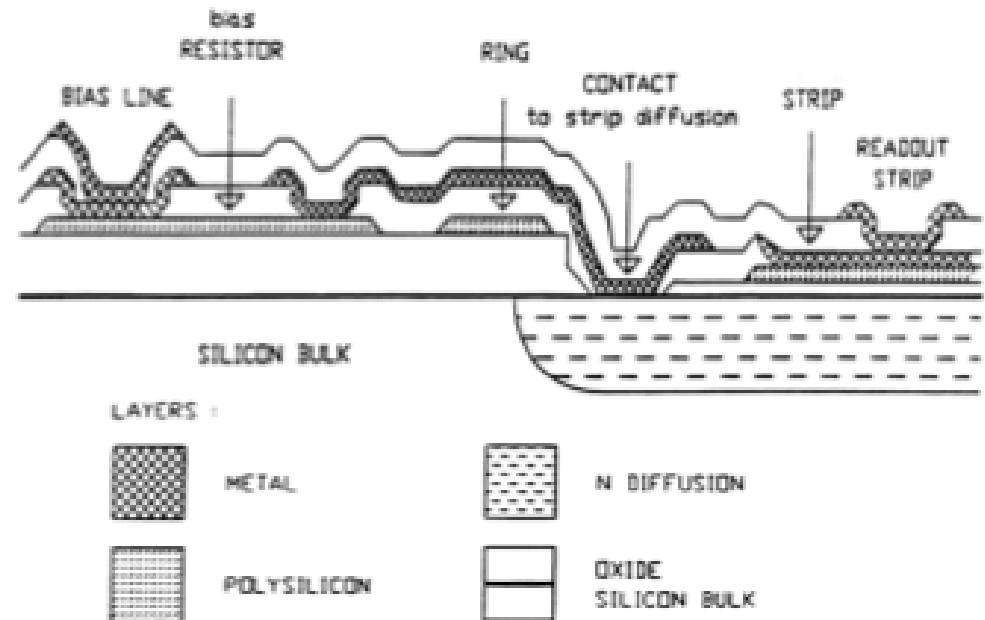


# 3. Double-sided double metal

3D scheme of an AC coupled double sided strip detector with 2<sup>nd</sup> metal readout lines (bias structure not shown). The isolation between the two metal layers is either polyimide or SiO<sub>2</sub>:



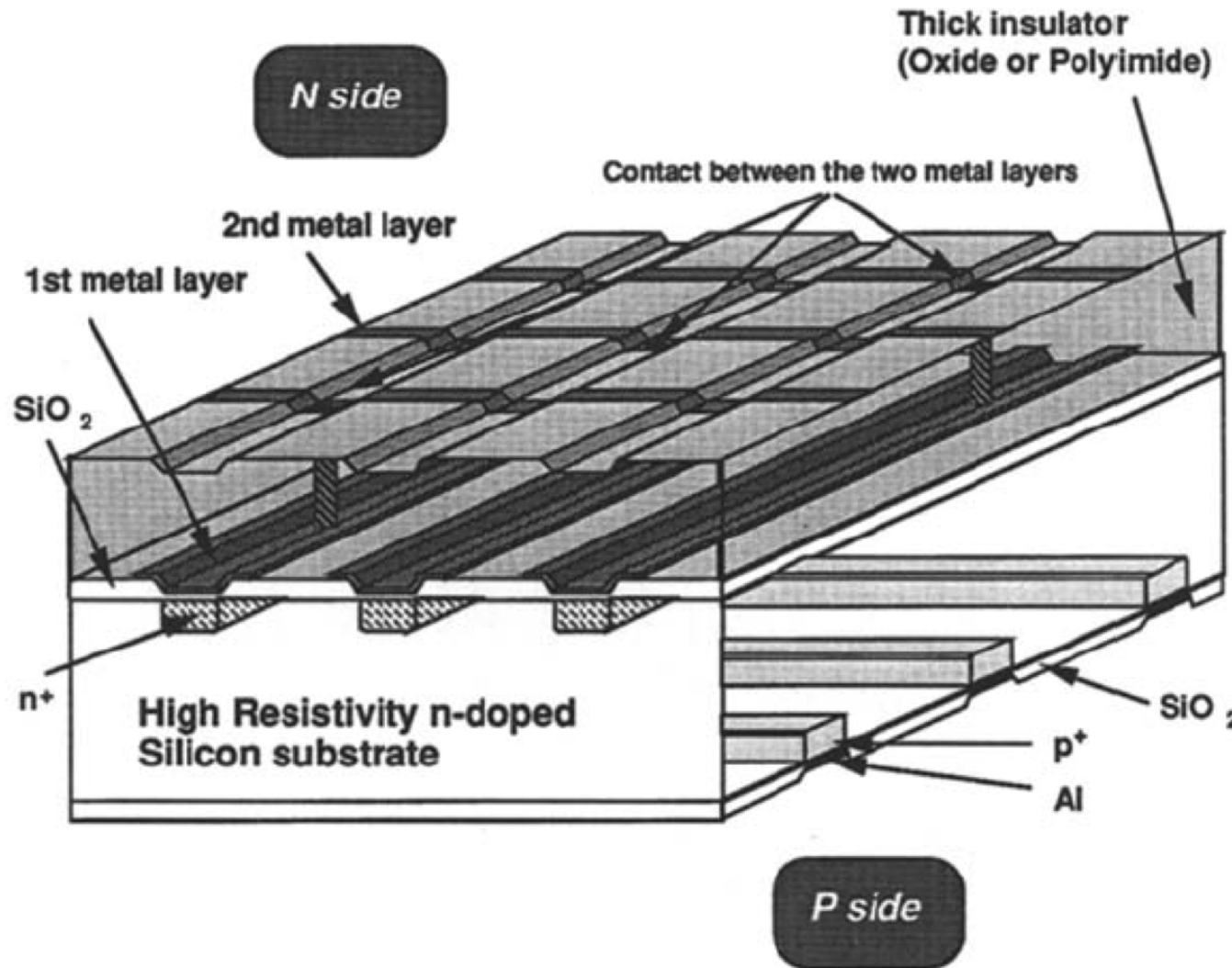
Cross section of the n<sup>+</sup> side of an AC coupled double sided strip detector with 2<sup>nd</sup> metal readout lines. Shown is the end of a strip with the bias resistor:



A. Peisert, *Silicon Microstrip Detectors*, DELPHI 92-143 MVX 2, CERN, 1992

# 3. Double-sided double metal

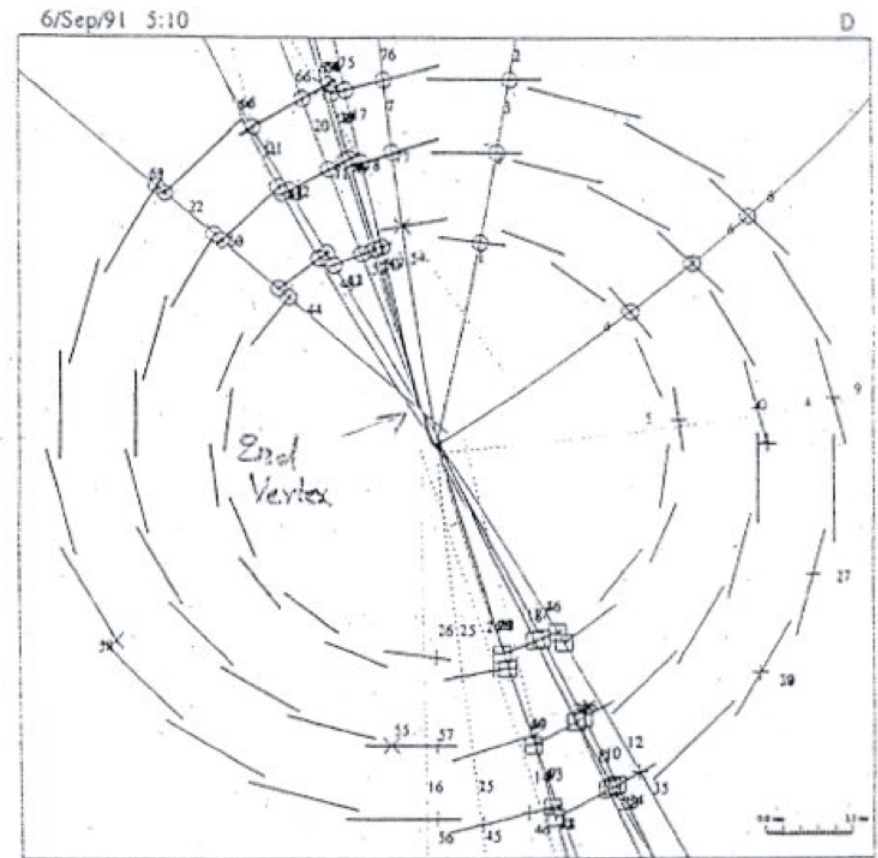
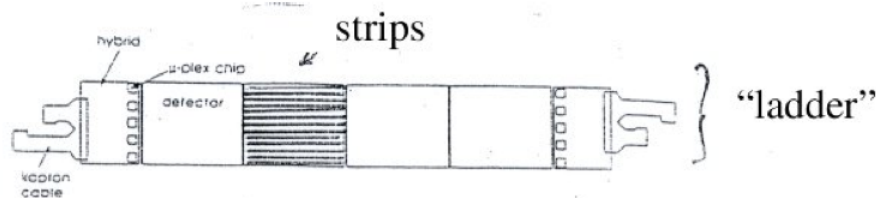
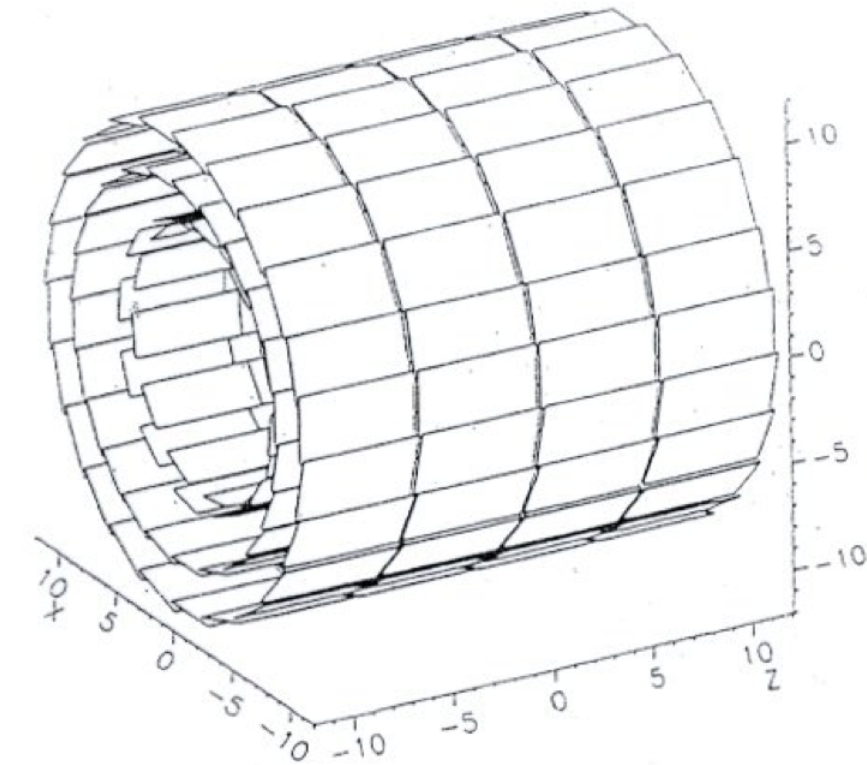
**My diploma thesis:** double-sided double-metal silicon microstrip detectors for the DELPHI experiment at LEP



# 3. Double-sided double metal

Initially: only single-sided detectors → only  $r\phi$  coordinate measured with high precision

3 coaxial layers of double-sided micro-strips, capacitive coupling, 6.3, 9.0, 10.9 cm from beam axis



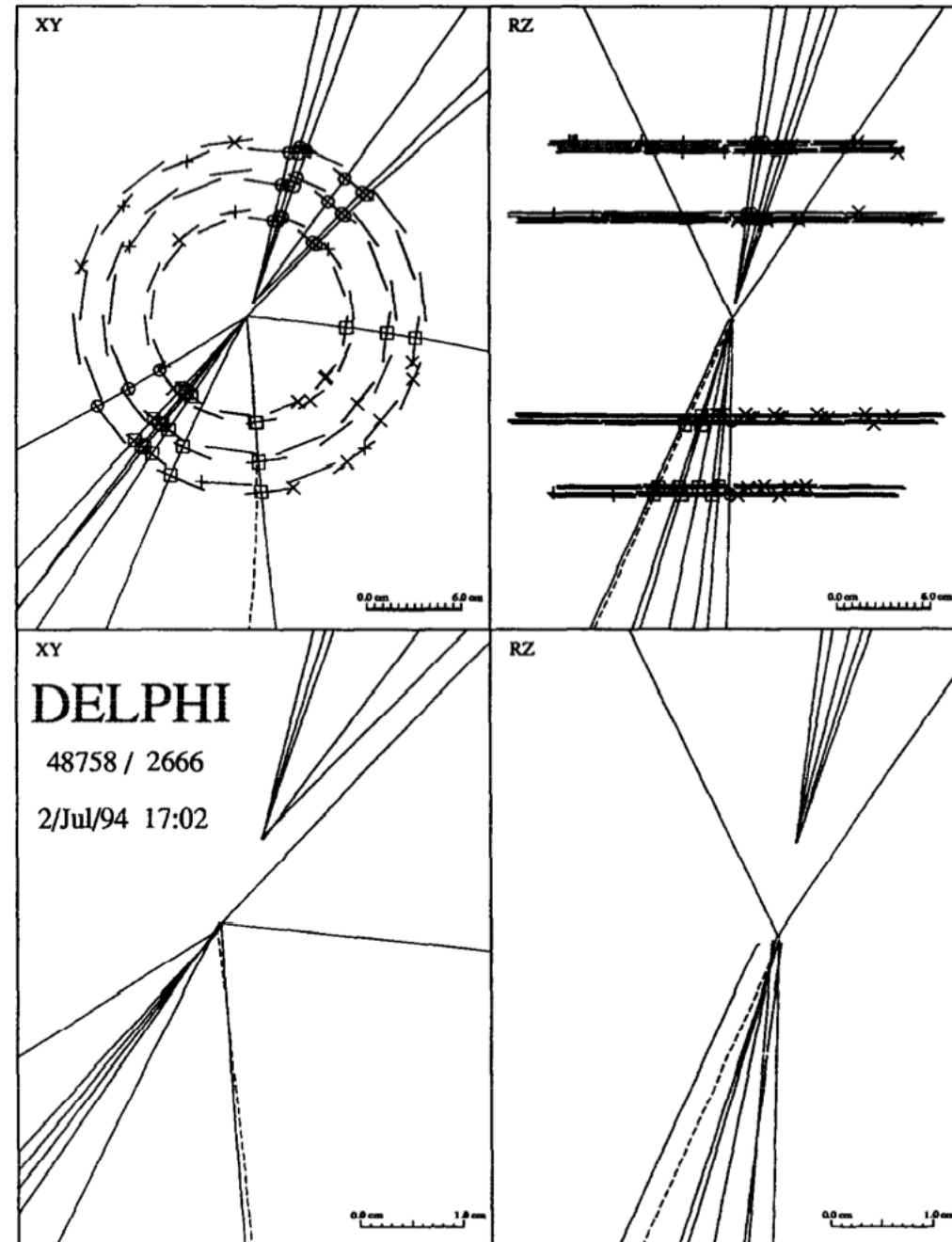
event recorded by the Delphi micro-vertex detector

# 3. Double-sided double metal

With the double-sided detectors → excellent resolution in rz also!

Very precise tracking in 3D → much more powerful reconstruction of secondary vertices!

V. Chabaud et al., *The DELPHI silicon strip microvertex detector with double sided readout*, NIM A 368 (1996) 314-332



## 4. Hybrid pixel detectors

Double sided strip sensors measure the 2 dimensional position of a particle track. However, if more than one particle hits the strip detector the measured position is no longer unambiguous. “Ghost”-hits appear!

True hits and ghost hits in a double sided strip detector in case of two particles traversing the detector:



Pixel detectors produce unambiguous hits!

Measured hits in a pixel detector in case of two particles traversing the detector:



Hybrid = 1 chip with the sensing pixels + 1 chip with the electronics

# 4. Hybrid pixel detectors

- Typical pixel size is 50  $\mu\text{m}$  x 50  $\mu\text{m}$ .
- If signal pulse height is not recorded, resolution is the digital resolution:

$$\sigma_x = \frac{d}{\sqrt{12}}$$

d = pixel dimension

~14  $\mu\text{m}$  (50  $\mu\text{m}$  pixel pitch)

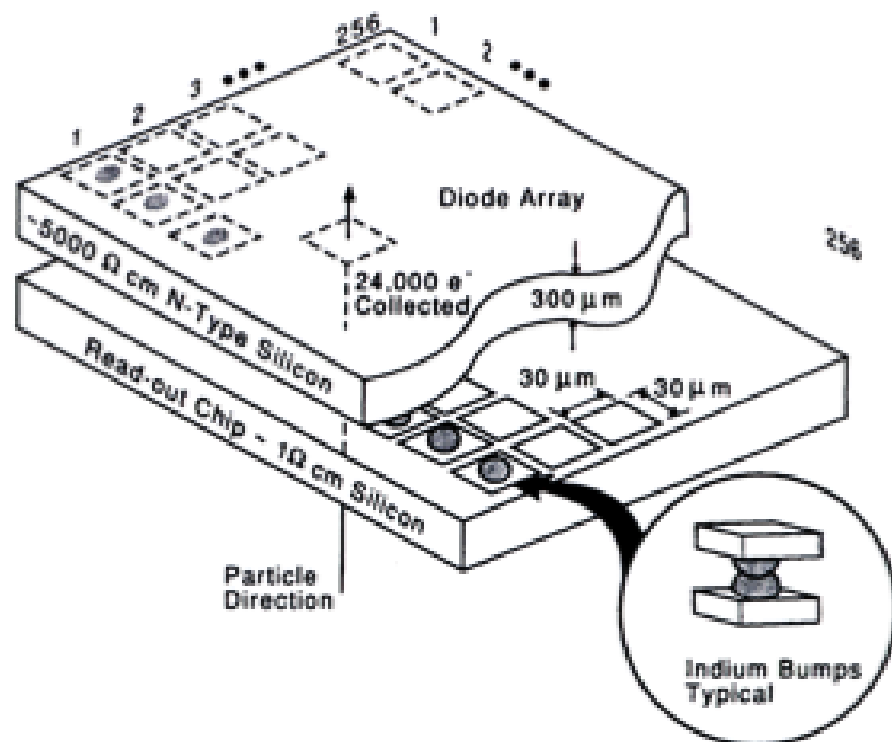
Better resolution achievable with analogue readout

- Small pixel area  $\rightarrow$  low detector capacitance ( $\approx 1$  fF/Pixel)  $\rightarrow$  large signal to-noise ratio (e.g. 150:1)
- Small pixel volume  $\rightarrow$  low leakage current ( $\approx 1$  pA/Pixel)
- Drawback of hybrid pixel detectors: Large number of readout channels
  - Large number of electrical connections in case of hybrid pixel detectors
  - Large power consumption of electronics..

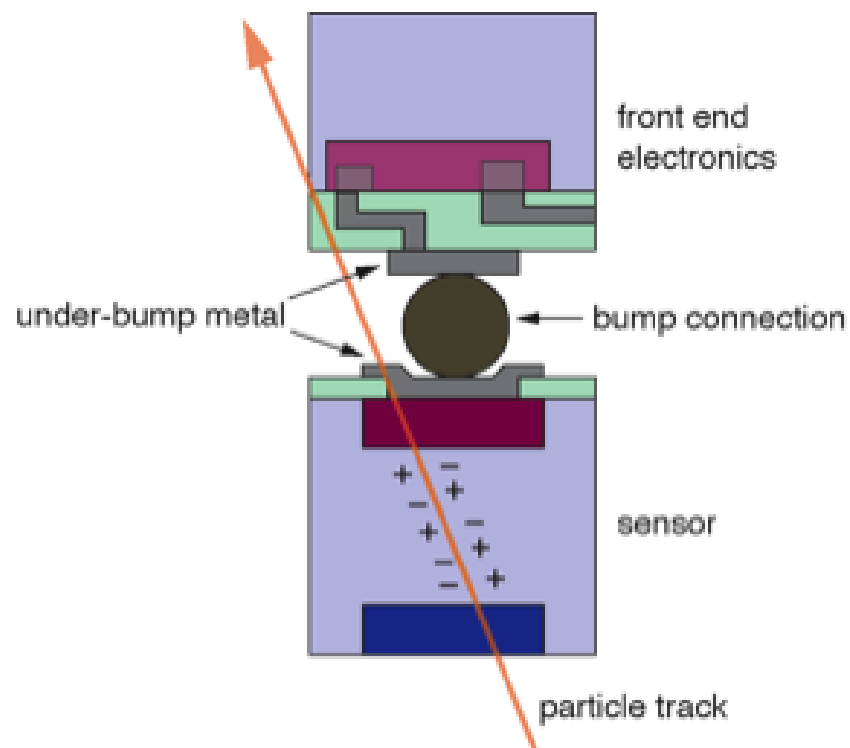
# 4. Hybrid pixel detectors

“Flip-Chip” pixel detector:

On top the Si detector, below the readout chip, bump bonds make the electrical connection for each pixel.



Detail of bump bond connection. Bottom is the detector, on top the readout chip:



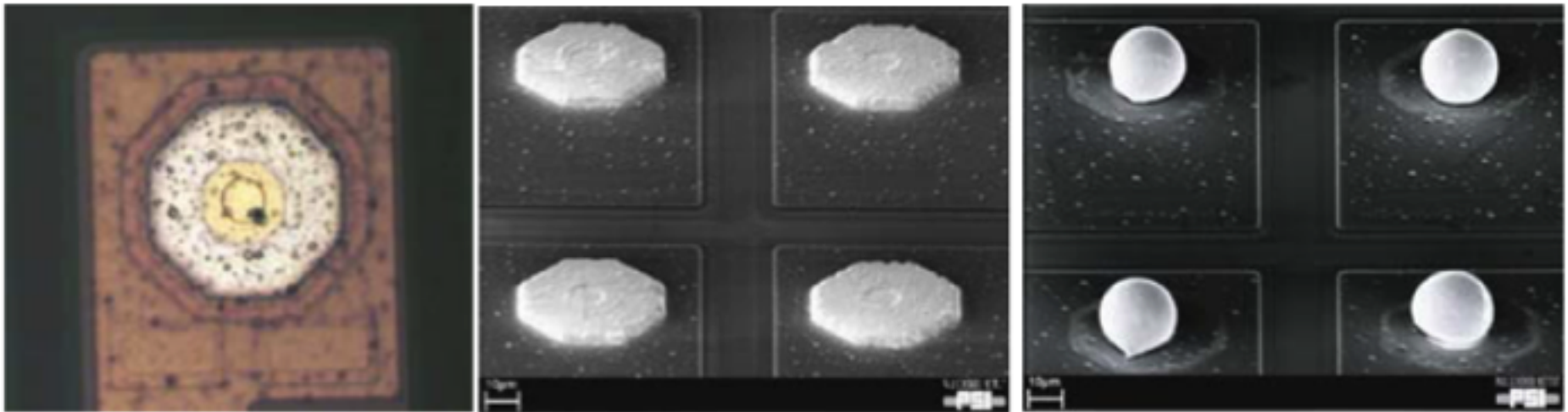
S.L. Shapiro et al., *Si PIN Diode Array Hybrids for Charged Particle Detection*, Nucl. Instr. Meth. A **275**, 580 (1989)

L. Rossi, *Pixel Detectors Hybridisation*, Nucl. Instr. Meth. A **501**, 239 (2003)

# 4. Hybrid pixel detectors

Electron microscope pictures before and after the reflow production step (where the deposited indium is re-shaped to form spheres).

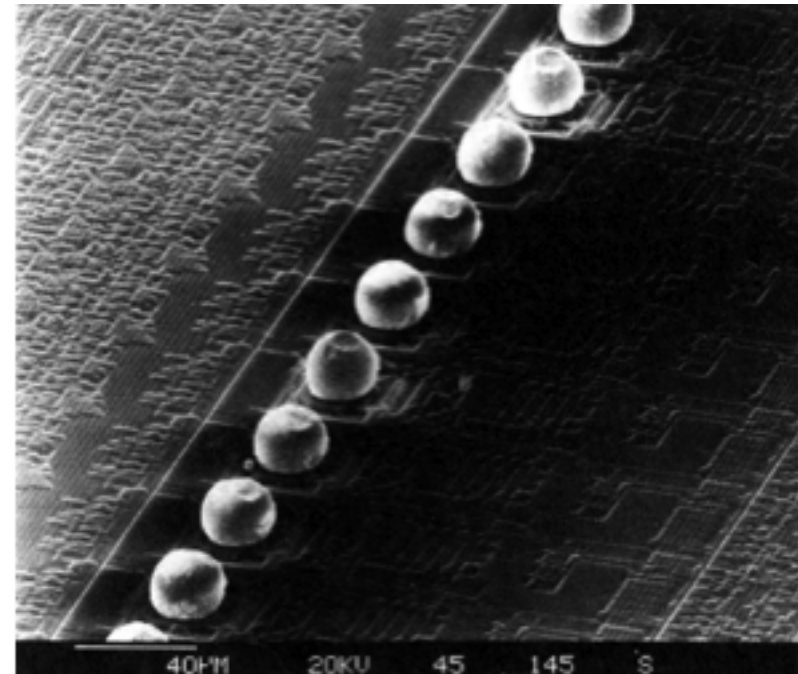
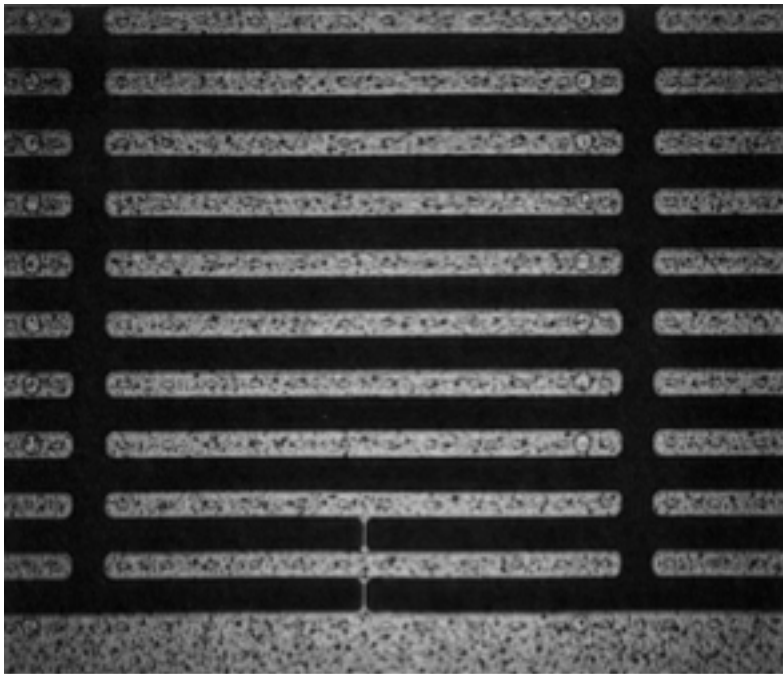
Indium bumps: The distance between bumps is  $100\ \mu\text{m}$ , the deposited indium is  $50\ \mu\text{m}$  wide while the reflowed bump is only  $20\ \mu\text{m}$  wide.



C. Broennimann, F. Glaus, J. Gobrecht, S. Heising, M. Horisberger, R. Horisberger, H. Kästli, J. Lehmann, T. Rohe, and S. Streuli, *Development of an Indium bump bond process for silicon pixel detectors at PSI*, *Nucl. Inst. Met. Phys. Res. A565(1)* (2006) 303–308 82

# 4. Hybrid pixel detectors

Electron microscope picture of pixel detector with long strip.  
Left: Detector chip, right: readout chip with bump bonds applied.



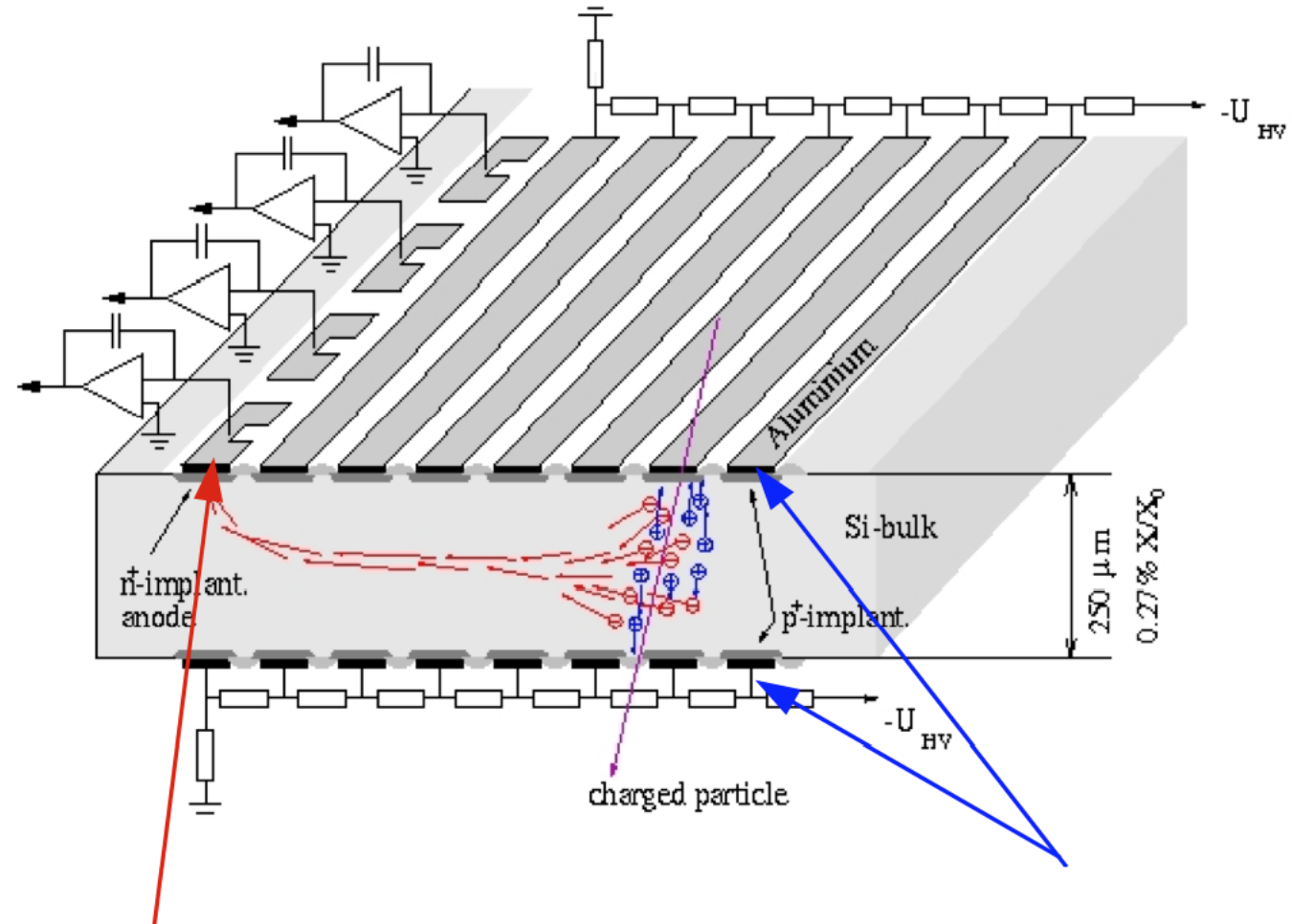
G. Lutz, *Semiconductor Radiation Detectors*, Springer-Verlag, 1999

# 5. Silicon drift detectors

Proposed by Gatti and Rehak in 1984, first realized in the 1990ies

p<sup>+</sup> strips and the backplane p<sup>+</sup> implantation are used to fully deplete the bulk. A drift field transports the generated electrons to the readout electrodes (n<sup>+</sup>).

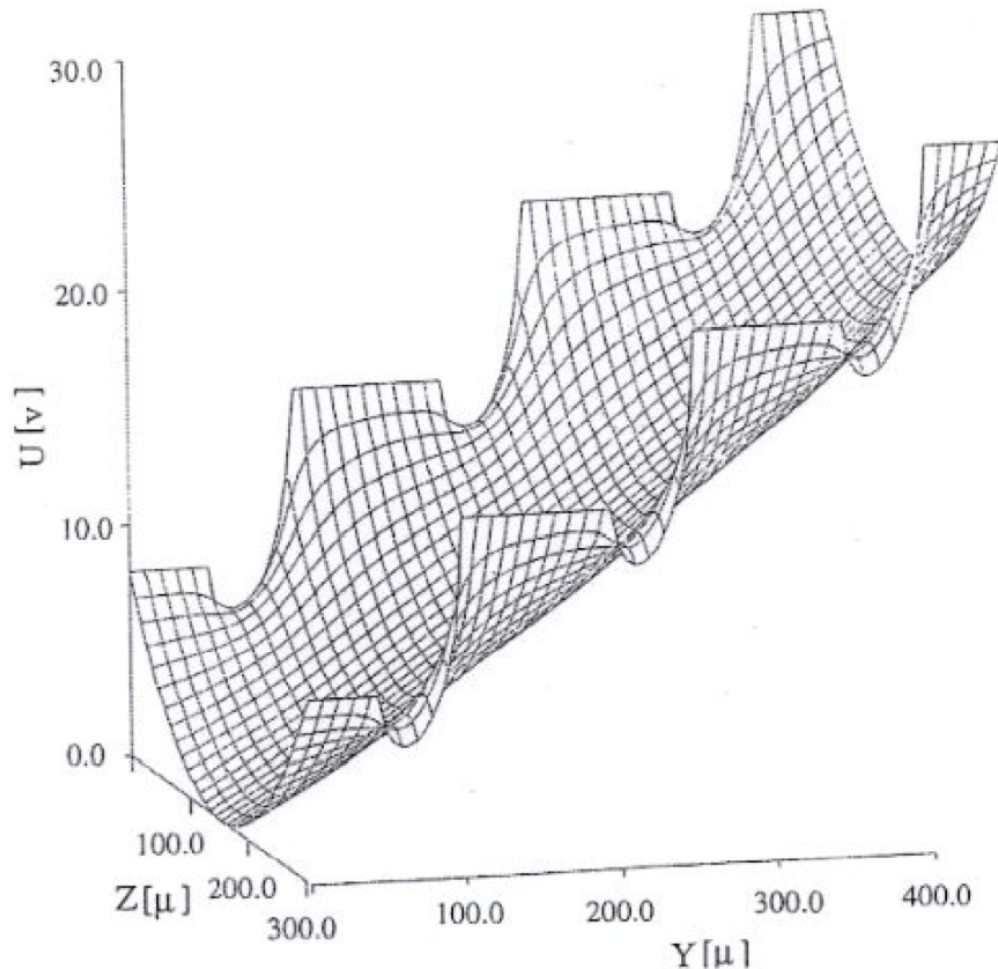
One coordinate is measured by signals on strips, the second by the drift time.



wafer can be fully depleted by reverse bias voltage on a small n<sup>+</sup> anode implanted on wafer edge

n-type bulk Si with p<sup>+</sup> electrodes on both flat sides

# 5. Silicon drift detectors



potential shape in Si drift-chamber:  
trough-like shape due to positive space charge in  
depletion area, slope from external voltage divider

Charge carriers drift in well  
defined E-field

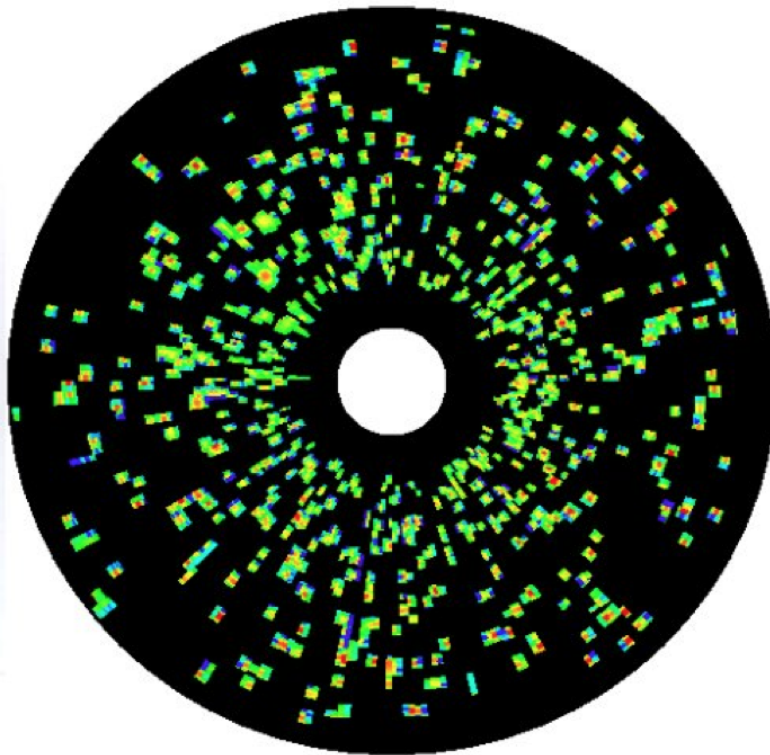
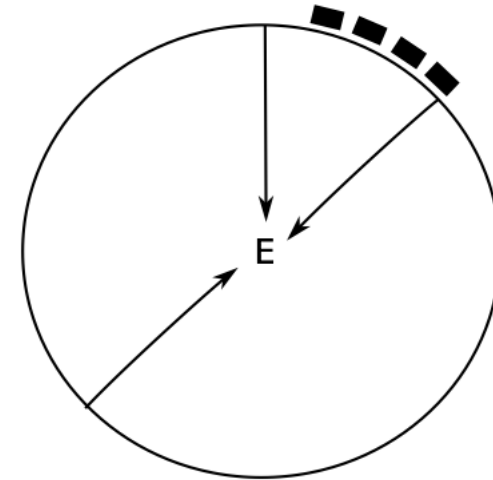
Measurement of drift time →  
position of ionizing particle

Typical drift time: a few  $\mu\text{s}$  for  
5-10 cm  
(relatively slow)

# 5. Silicon drift detectors: CERES

First example: CERES at the SPS:  
Radial silicon drift detector (4" wafers)

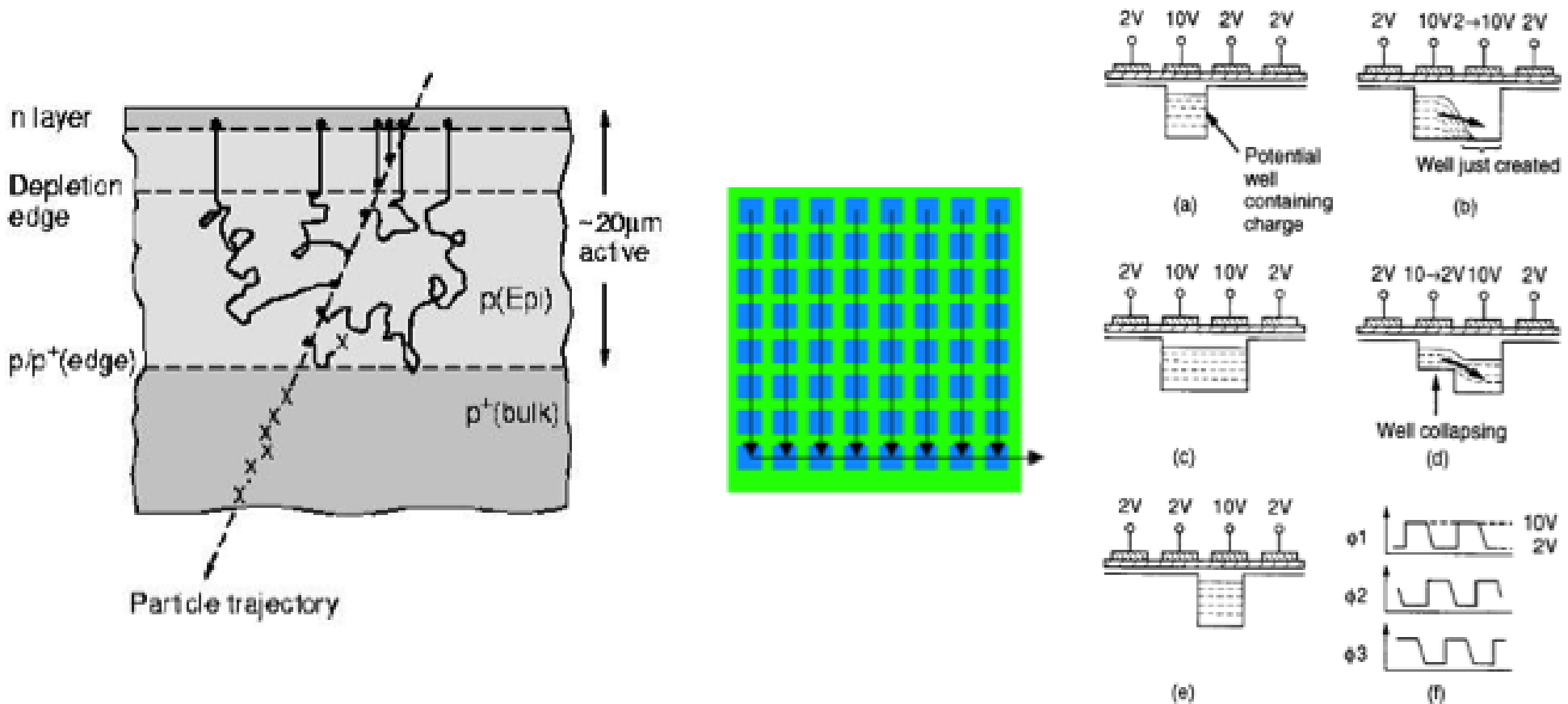
Event display:



active area	52 cm <sup>2</sup>
granularity	360 anodes × 256 time bins = 92 160 pixels
max. number of resolved hits	$2 \cdot 10^4$
wafer thickness	250 μm
radiation length	0.27% of X <sub>0</sub>
multiple scattering	≈ 0.54 mrad @ 1 GeV/c

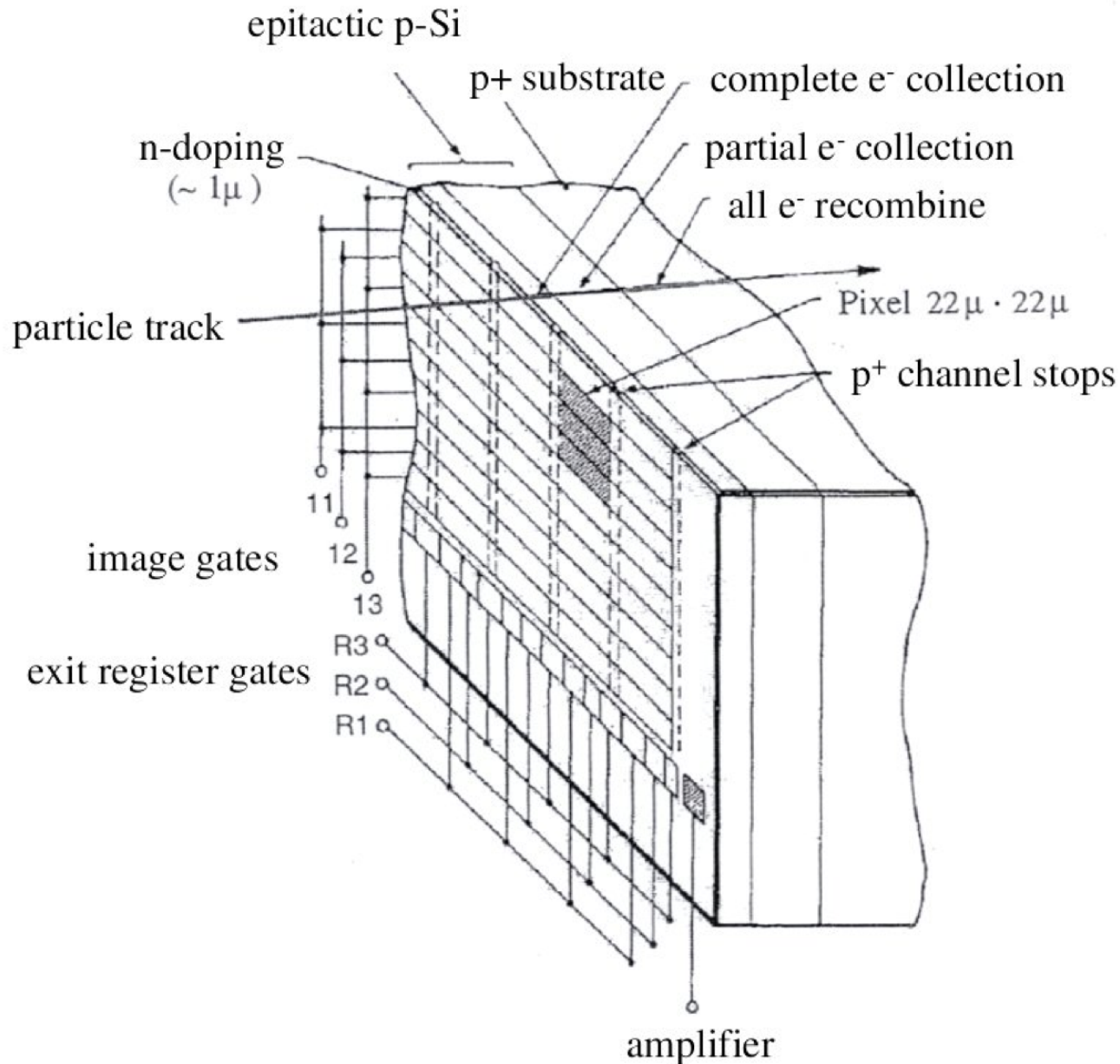
# 6. Charge-coupled devices (CCD)

Shallow depletion layer (typically 15  $\mu\text{m}$ ), relatively small signal, the charge is kept in the pixel and during readout shifted through the columns and through final row to a single signal readout channel:



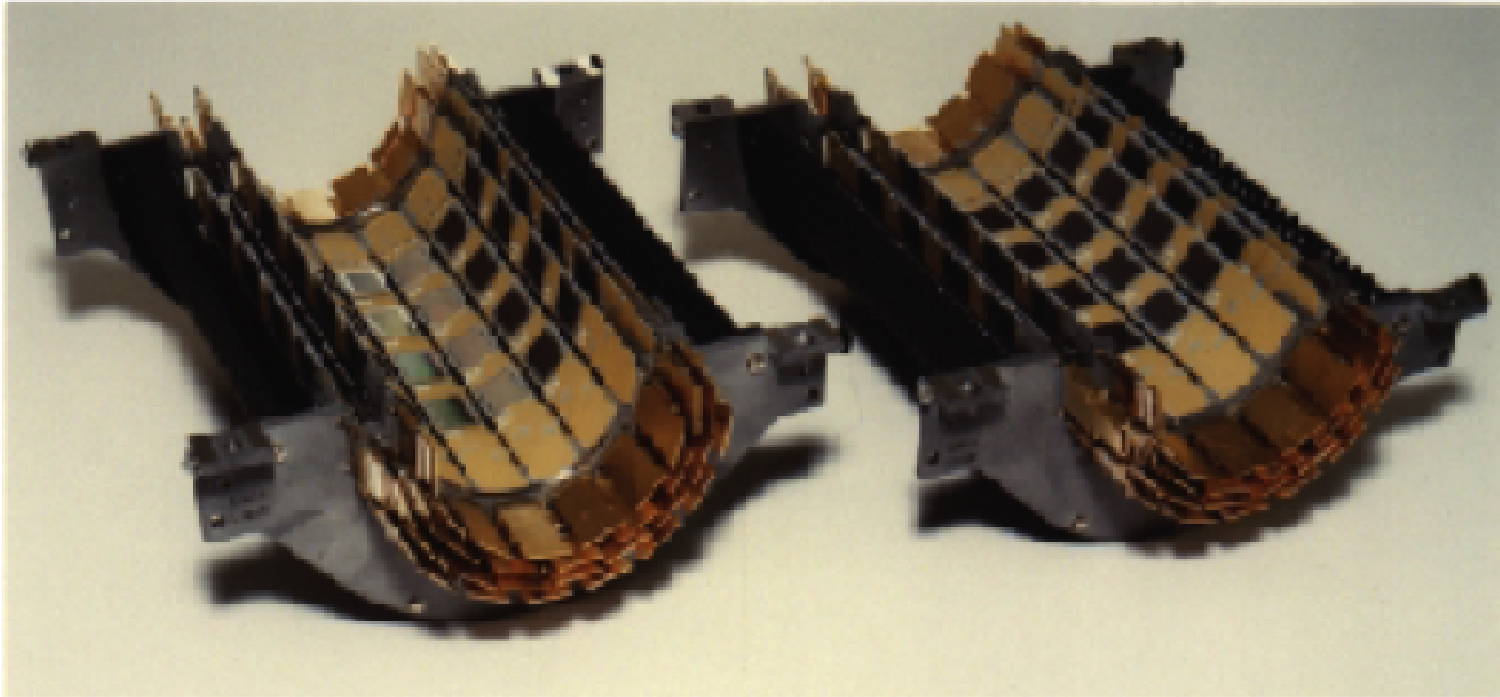
Slow device, hence not suitable for fast detectors.  
Improvements are developed, e.g. parallel column readout.

# 6. Charge-coupled devices (CCD)



## 6. Charge-coupled devices (CCD): SLD

The SLD (SLAC, USA) silicon vertex detector used large area CCDs. Pixel size  $20\ \mu\text{m} \times 20\ \mu\text{m}$ , achieved resolution  $4\ \mu\text{m}$ .



# 6. Charge-coupled devices (CCD)



## The Nobel Prize in Physics 2009

**"For groundbreaking achievements concerning the transmission of light in fibers for optical communication"**

**"For the invention of an imaging semiconductor circuit – the CCD sensor"**



Photo: U. Montan

**Charles K. Kao**

1/2 of the prize



Photo: U. Montan

**Willard S. Boyle**

1/4 of the prize



Photo: U. Montan

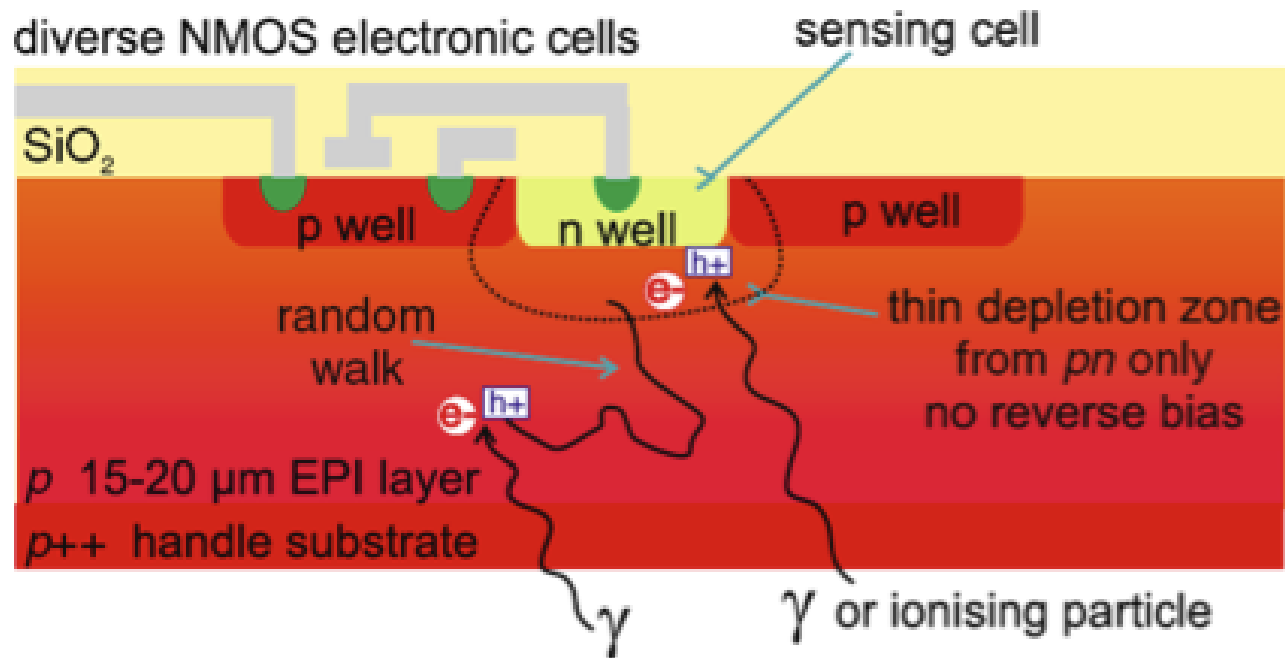
**George E. Smith**

1/4 of the prize

# 7. Monolithic active pixel sensors (MAPS)

## CMOS

Scheme of a CMOS monolithic active pixel cell with an NMOS transistor. The N-well collects electrons from both ionization and photo-effect.

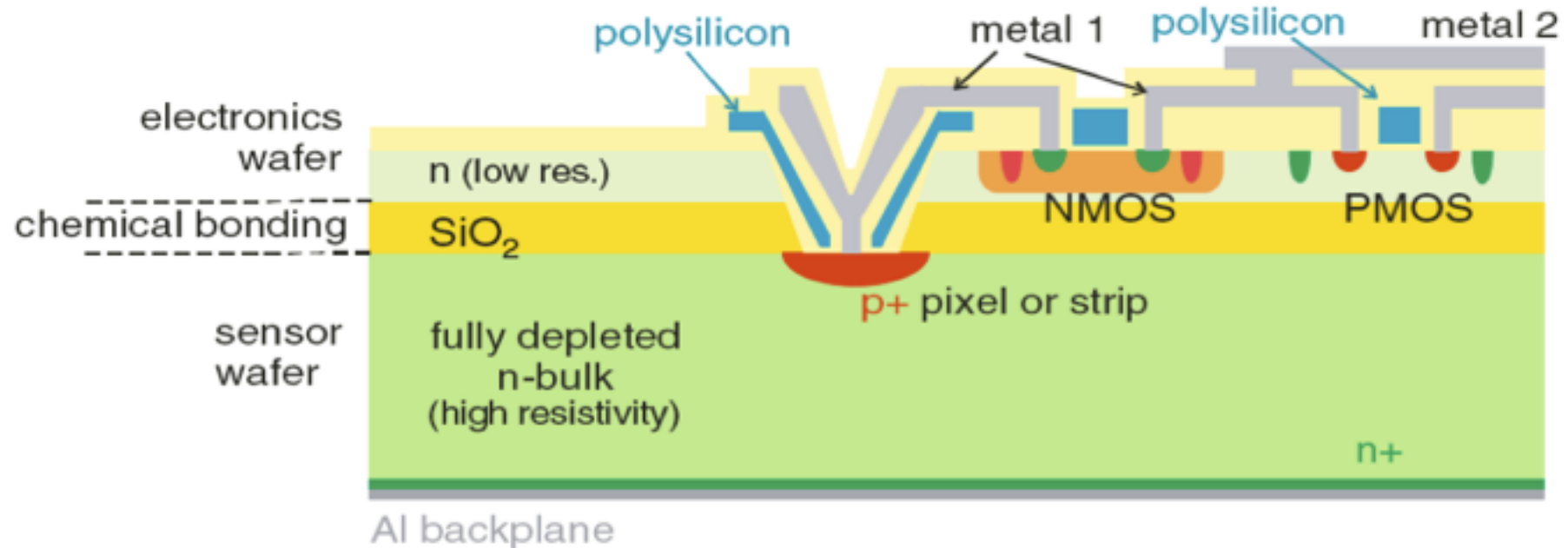


Evolution of Silicon Sensor Technology in Particle Physics, F. Hartmann, Springer Volume 231, 2009

# 7. Monolithic active pixel sensors (MAPS)

## SOI: Silicon On Insulator

A SOI detector consists of a thick full depleted high resistivity bulk and, separated by a layer of  $\text{SiO}_2$ , a low resistivity n-type material. NMOS and PMOS transistors are implemented in the low resistivity material using standard IC methods.

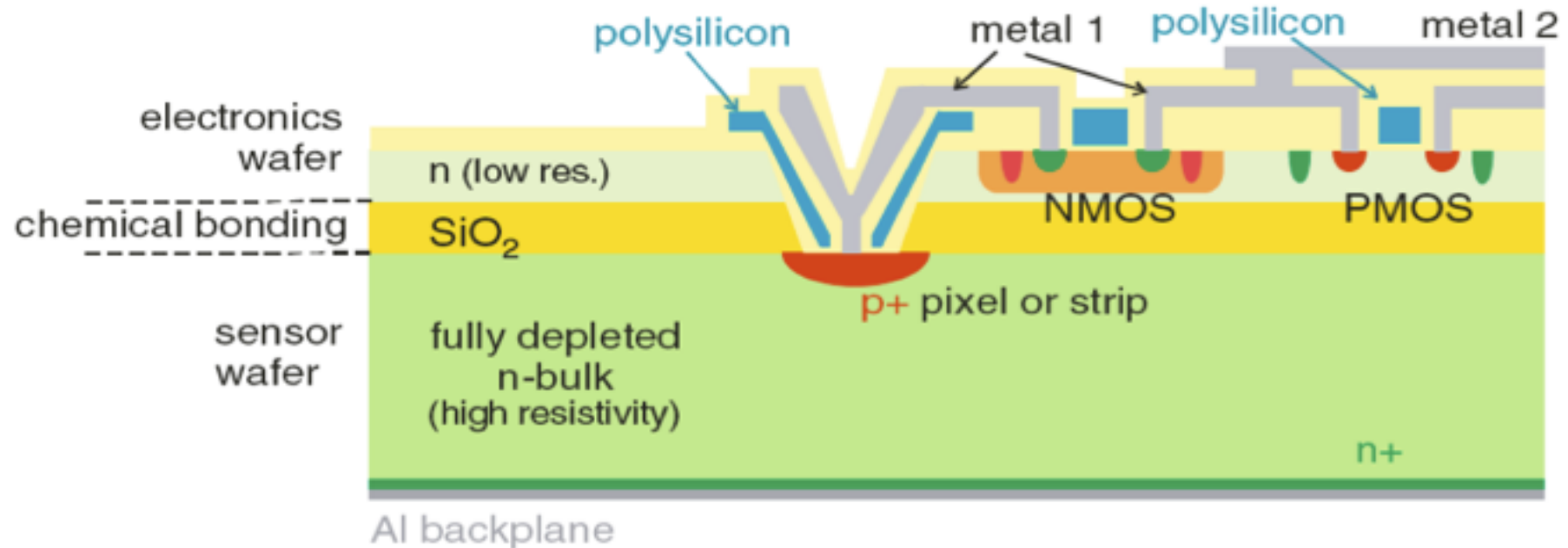


Evolution of Silicon Sensor Technology in Particle Physics, F. Hartmann, Springer Volume 231, 2009

# 7. Monolithic active pixel sensors (MAPS)

## SOI: Silicon On Insulator

A SOI detector consists of a thick full depleted high resistivity bulk and, separated by a layer of  $\text{SiO}_2$ , a low resistivity n-type material. NMOS and PMOS transistors are implemented in the low resistivity material using standard IC methods.



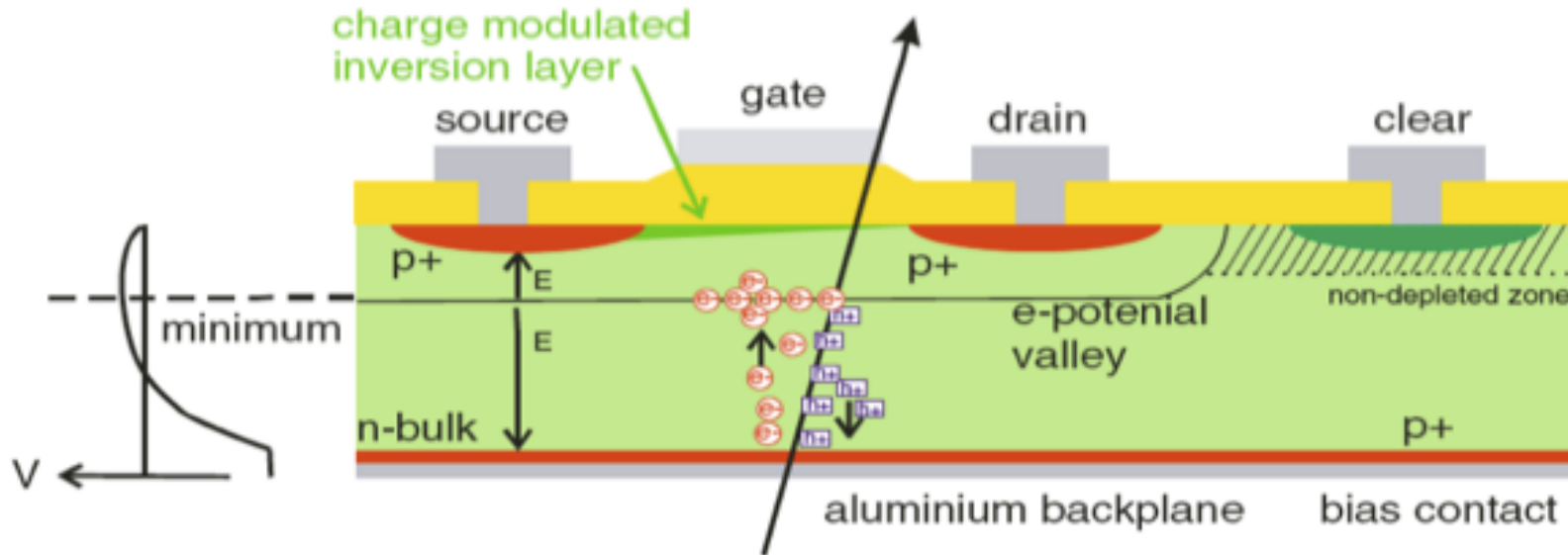
Evolution of Silicon Sensor Technology in Particle Physics, F. Hartmann, Springer Volume 231, 2009

# 8. DEPFET detectors

The DEPFET detector is a detector with an internal amplification structure.

The n-bulk is fully depleted with a potential minimum below the strips and the structure of a field effect transistor. The electrons created by a charged particle accumulate in the potential minimum. The field configuration is such that the electrons drift underneath the gate of the transistor modifying the source drain current. An active clear is necessary to remove the electrons.

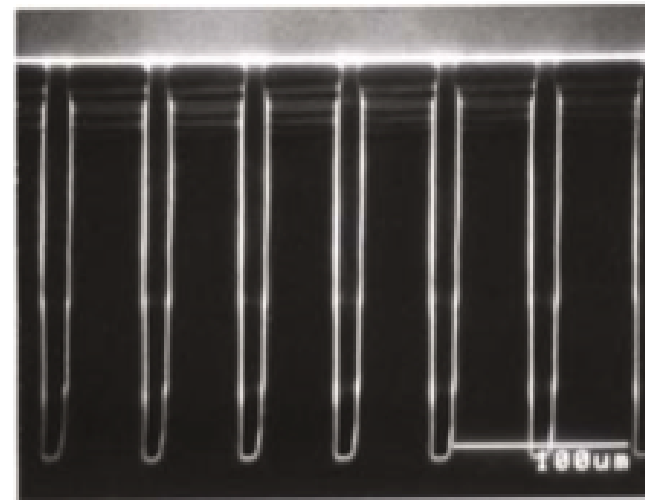
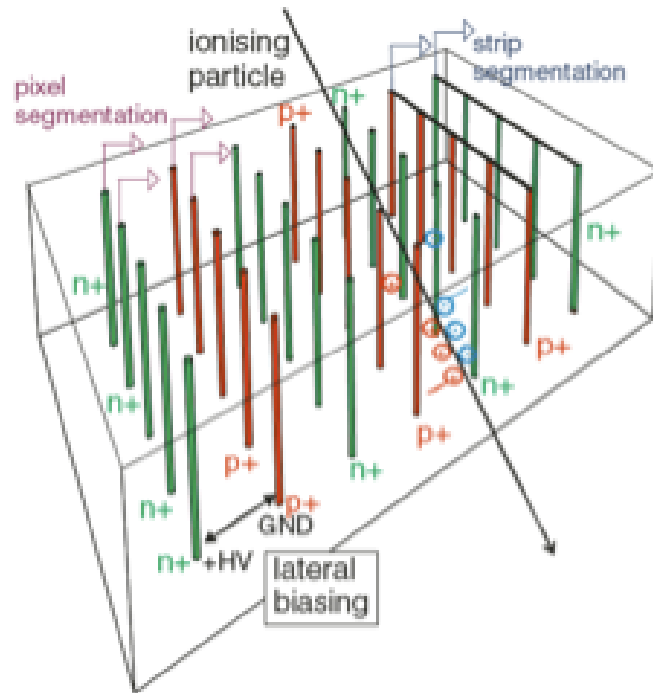
Used in Belle II and candidate for ILC



Evolution of Silicon Sensor Technology in Particle Physics, F. Hartmann, Springer Volume 231, 2009  
J. Kemmer and G. Lutz, NIM A253 (1987) 365

# 9. 3D detectors

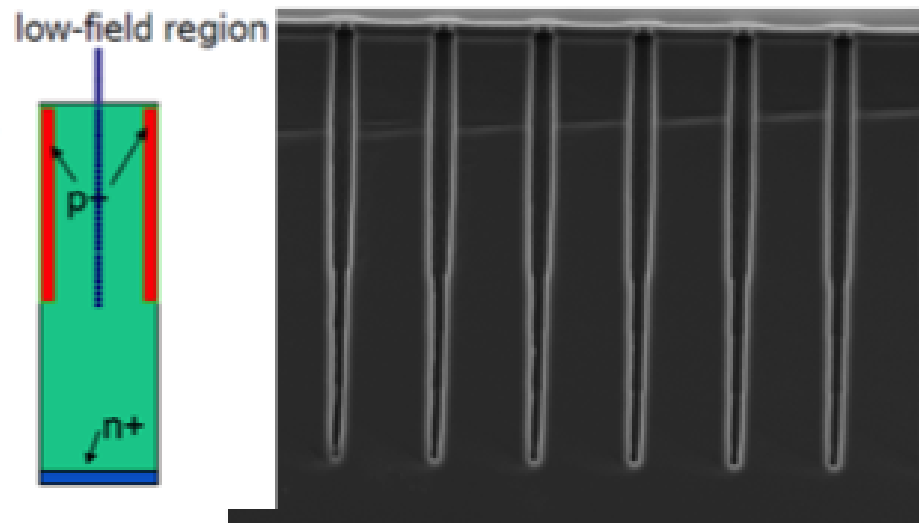
3D detectors are non planar detectors. Deep holes are etched into the silicon and filled with  $n^+$  and  $p^+$  material. Depletion is sideways. The distances between the electrodes are small, hence depletion voltage can be much smaller and charge carriers travel much short distances.



Very radiation tolerant detectors, first use in ATLAS IBL layer.

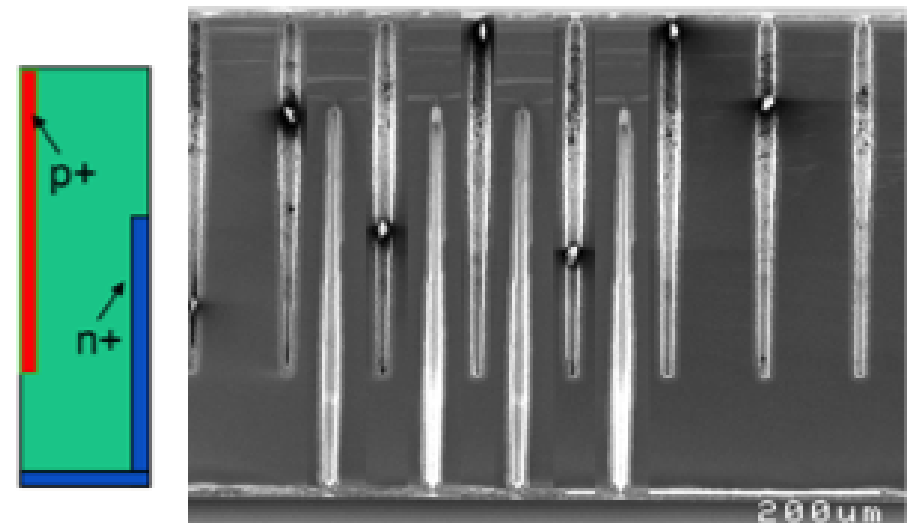
# 9. 3D detectors: different approaches

Single column:



Low field region between columns

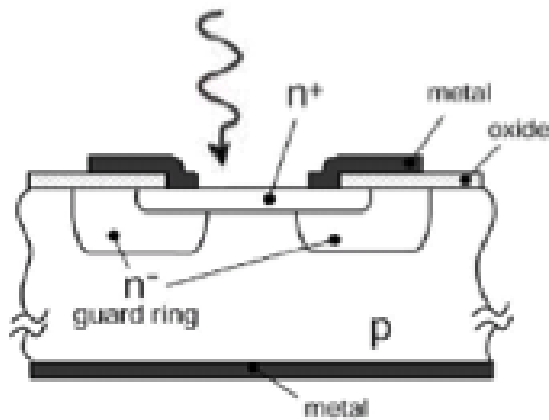
Double-sided double column:



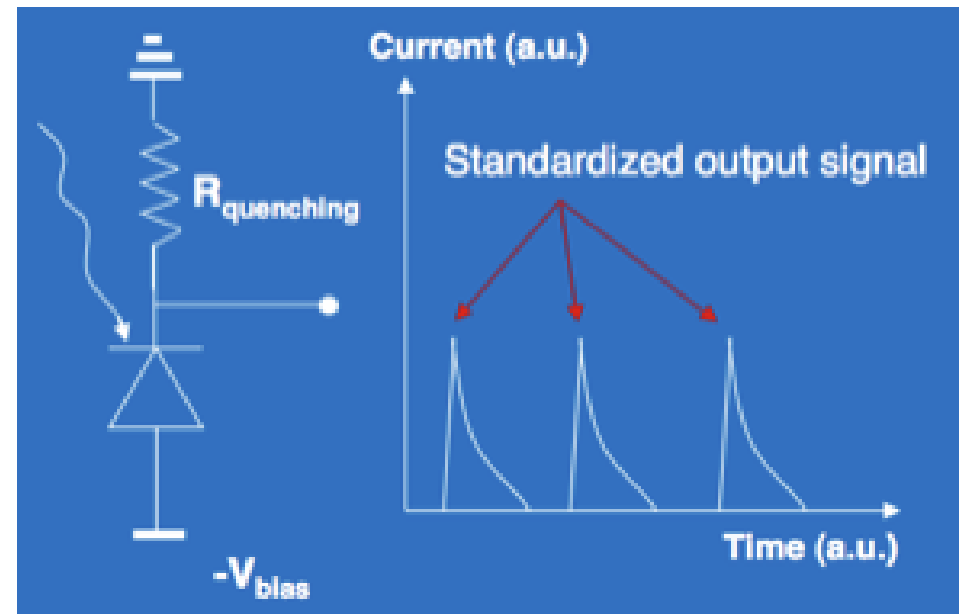
High field, but more complicated

# 10. Avalanche photo-diodes (APD)

APD are operated in reverse bias mode in the breakdown regime. A photon is able to trigger an avalanche breakdown. The current increase has to be limited by a quenching resistor.



R. H. Haitz, J. App.Phys. Vol. 36, No. 10 (1965) 3123

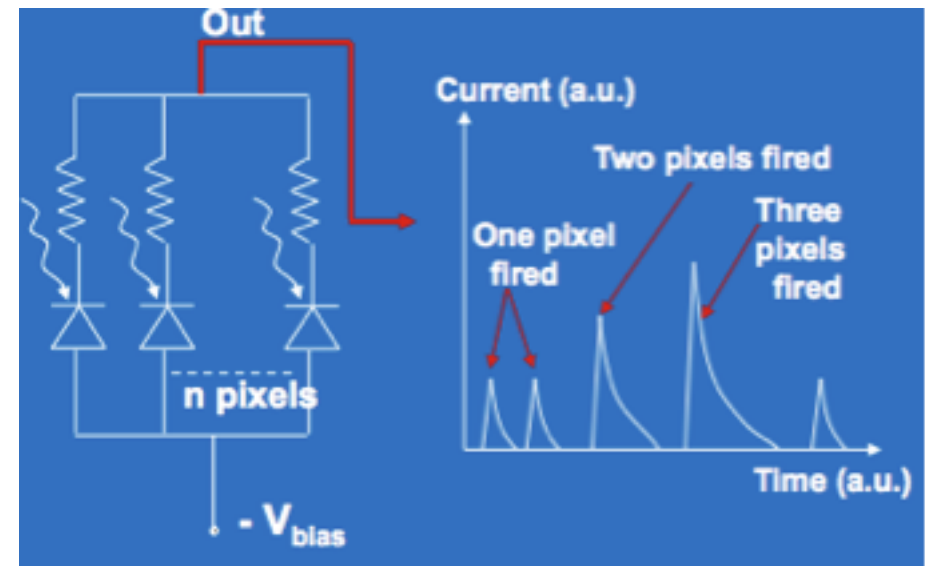
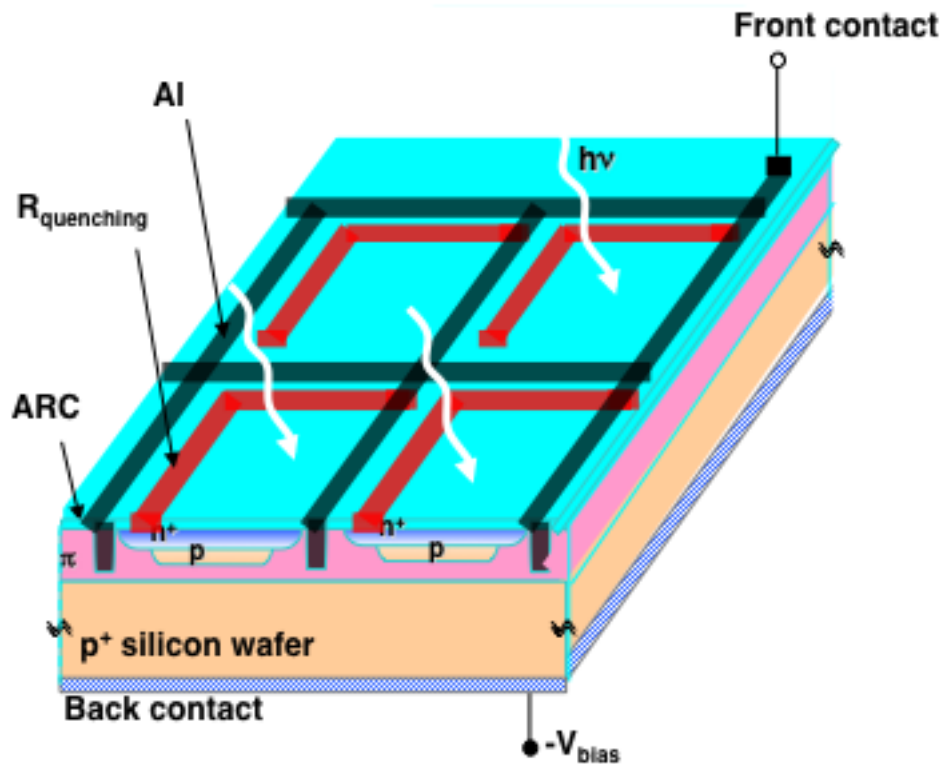


Used for photon detection in calorimeters (e.g the electromagnetic calorimeter of CMS), in cherenkov counters, etc.

# 10. Avalanche photo-diodes (APD)

Silicon Photo Multiplier (SiMP)

SiPM are matrices of APDs:



SiPM become more and more popular as replacement for standard photo multipliers

# RADIATION DAMAGE

# Radiation damage: motivation

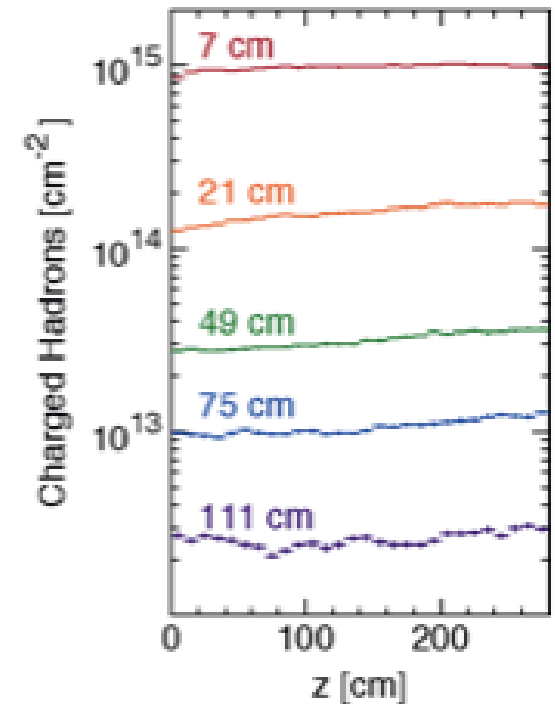
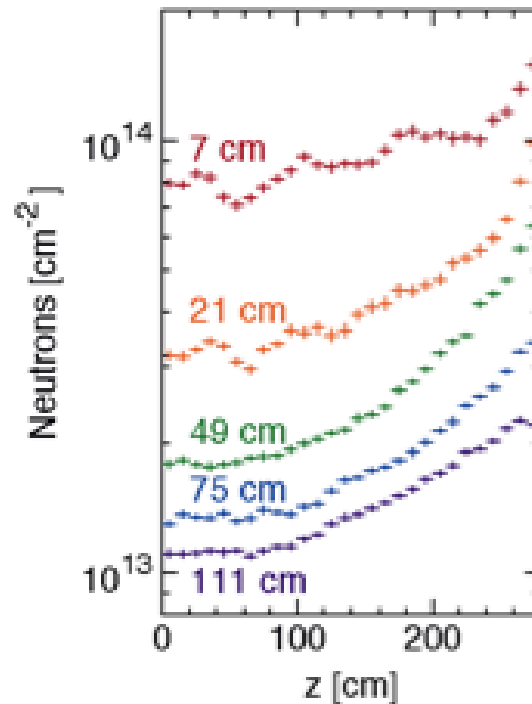
The event rate and as a consequence the irradiation load in experiments at hadron colliders is extreme (e.g. the pp collider LHC, collision energy 14 TeV, event rate =  $10^9$  /s).

Silicon detectors are the closest to the interaction point!

Expected particle rates for the silicon detector inner layers in CMS integrated over 10 years as a function of the distance from the vertex point and for various radii.

Left: neutrons

Right: charged hadrons



CERN/LHCC 98-6, CMS TDR 5, 20 April 1998

# Radiation damage: introduction

- Particles (radiation) interact
  - with the electrons: used for particle detection and results in temporarily effects only.
  - with atoms of the detector material: may cause permanent changes (defects) in the detector bulk.
- One distinguishes between damage inside the detector bulk (**bulk damage**) and damage introduced in the surface layers (**surface damage**).

For the readout electronics (also silicon based!) inside the radiation field only surface damage is relevant.
- Defects may change with time. Therefore one distinguishes also between **primary defects and secondary defects**. The secondary defects appear with time caused by moving primary defects.

# Radiation damage: introduction

---

- Radiation induced damage in the semiconductor **bulk** are dislocated atoms from their position in the lattice. Such dislocations are caused by massive particles.
  - Bulk damage is primarily produced by **neutrons, protons and pions.**
- In the amorphous **oxide** such dislocations are not important. The radiation damage in the oxide is due to the charges generated in the oxide. Due to the isolating character of the oxide these charges cannot disappear and lead to local concentrations of these charges.
  - Radiation damage in the oxide is primarily produced by **photons and charged particles.**

# Radiation damage: introduction

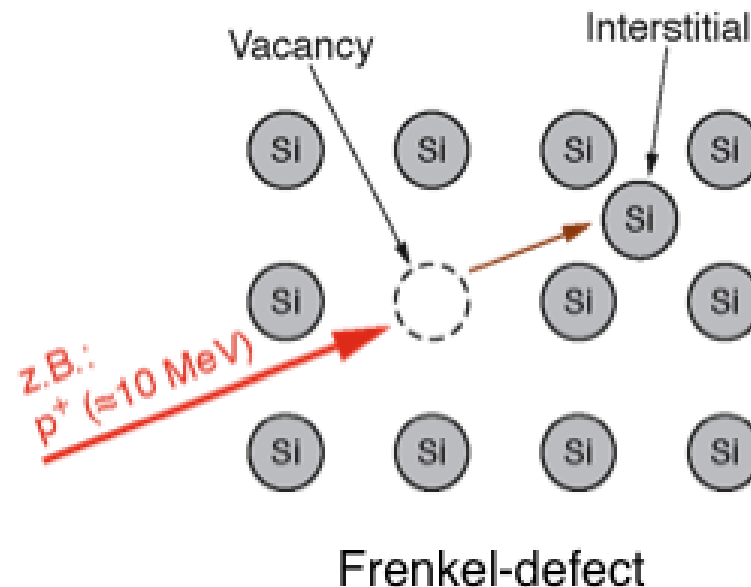
- Defects in the semiconductor lattice create energy levels in the band gap between valence and conduction band
- Depending on the position of these energy levels the following effects will occur:
  1. **Modification of the effective doping concentration**  
shift of the value of the depletion voltage.  
This effect is caused by shallow energy levels (close to the band edges).
  2. **Trapping of charge carriers**  
reduced lifetime of charge carriers  
Mainly caused by deep energy levels.
  3. **Easier thermal excitation of  $e^-$  and  $h^+$**   
increase of the leakage current  
Responsible are mainly levels in the middle of the band gap.

# Radiation damage: defects

## Point defect

A displaced silicon atom produces an empty space in the lattice (**Vacancy, V**) and in another place an atom in an inter lattice space (**Interstitial, I**).

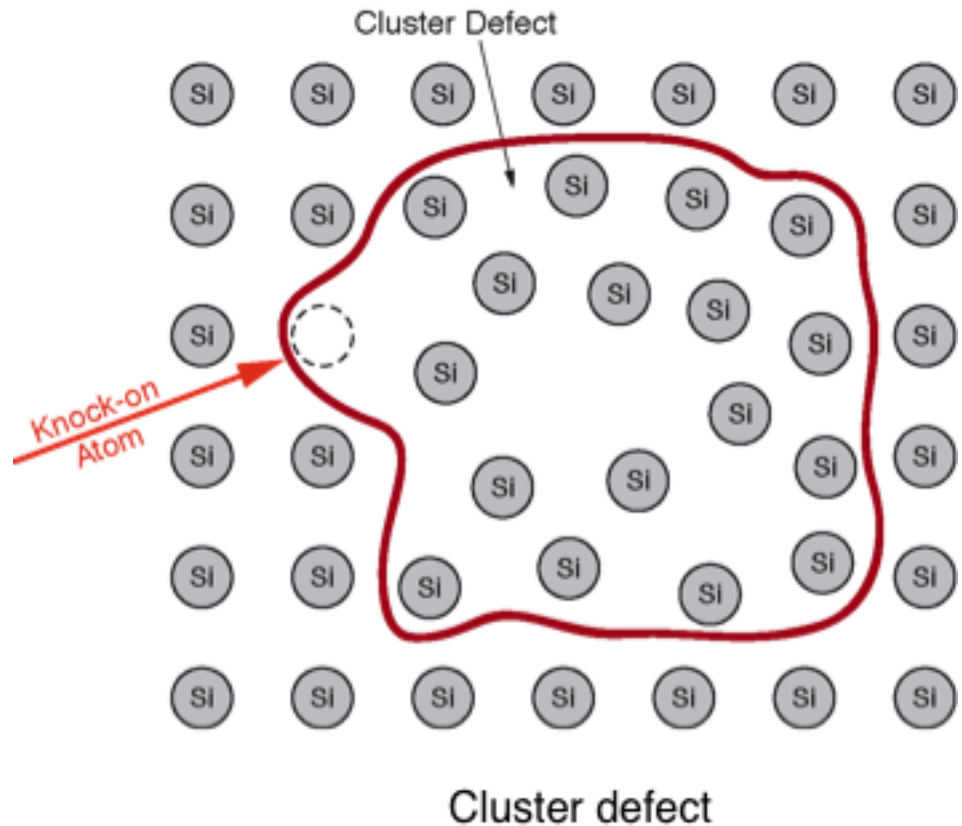
A vacancy-interstitial pair is called a **Frenkel-defect**.



# Radiation damage: defects

## Cluster defect

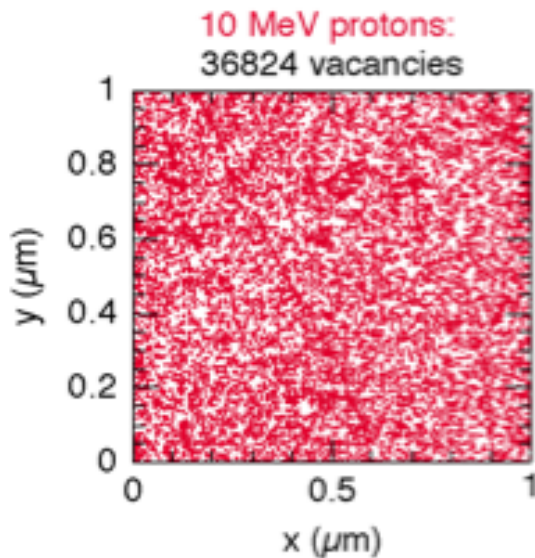
- In hard impacts the primary knock-on atom (PKA) displaces additional atoms. These defects are called cluster defects.
- The size of a cluster defect is approximately 5 nm and consists of about 100 dislocated atoms.
- For high energy PKA cluster defects appear at the end of the track when the atom loses the kinetic energy and the elastic cross section increases.



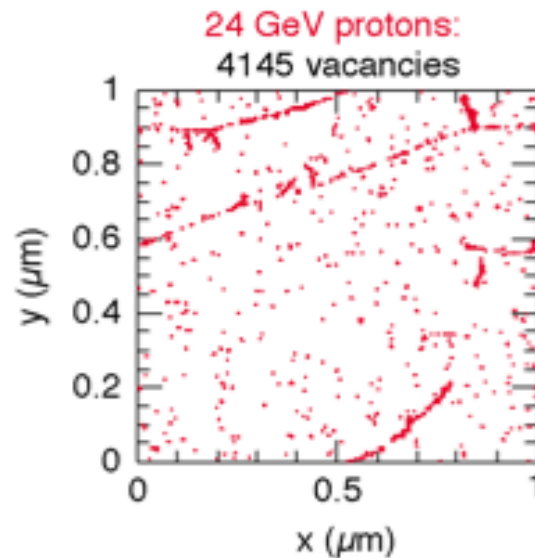
# Radiation damage: defects

Type and frequency of defects depends on the particle type and the energy.

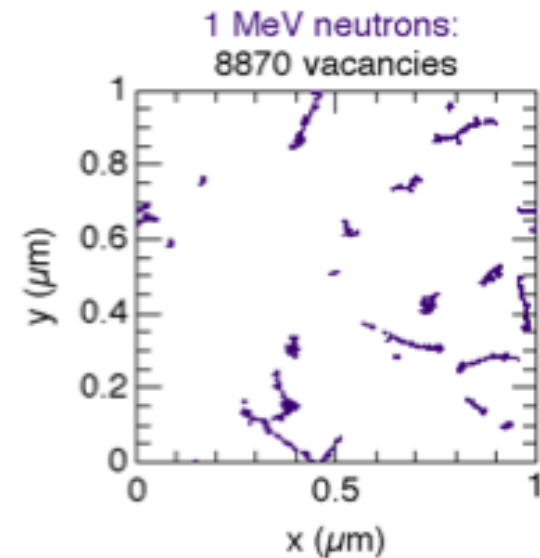
Plots below show a simulation of vacancies in 1  $\mu\text{m}$  thick material after an integrated flux of  $10^{14}$  particles /  $\text{cm}^2$ :



Many vacancies produced



Less vacancies, a significant part of the energy is consumed to produce cluster defects



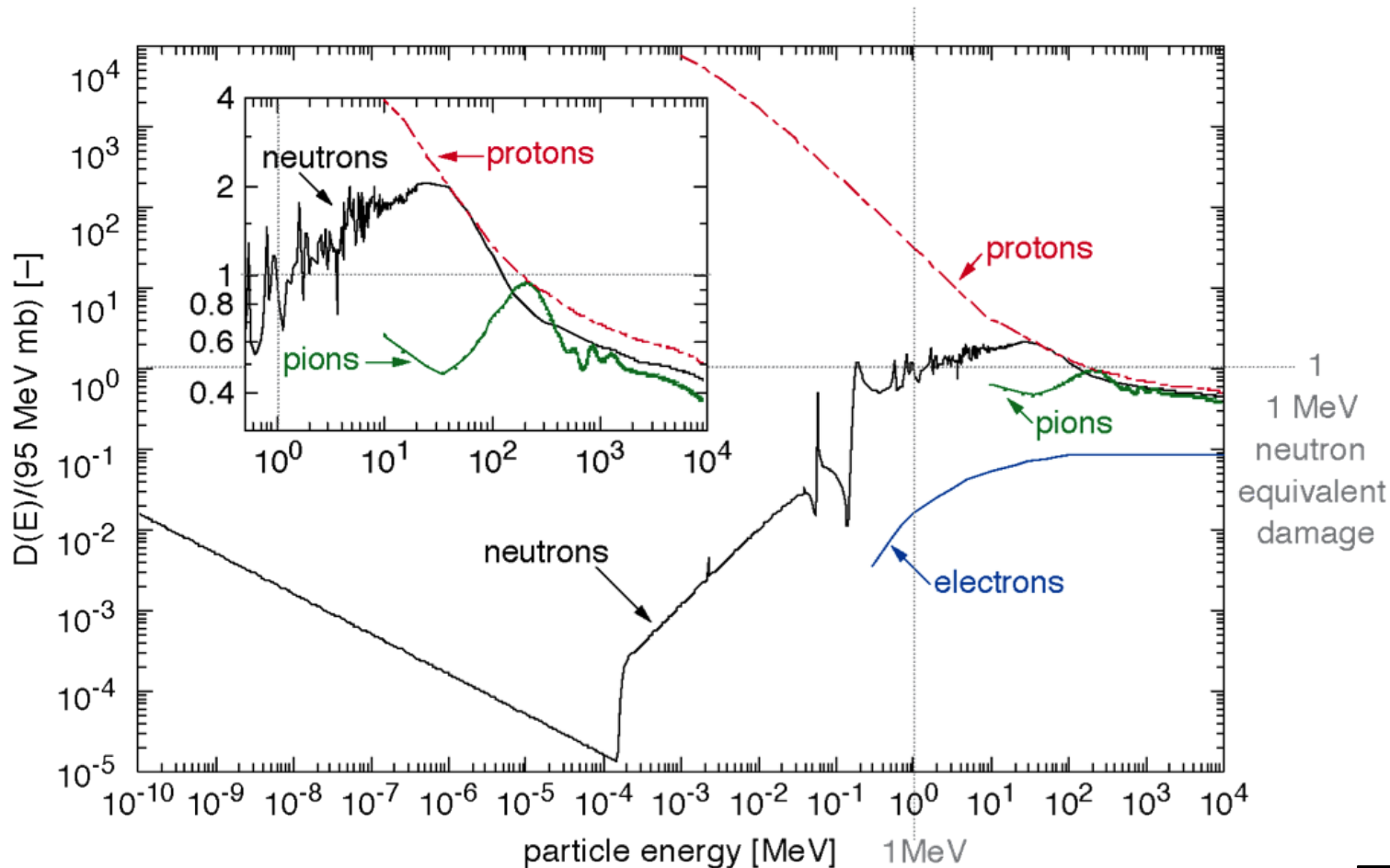
Very few vacancies, energy of the neutrons is used up to produce cluster defects.

M. Huhtinen, *Simulation of Non-Ionising Energy Loss and Defect Formation in Silicon*, Nucl. Instr. Meth. A **491**, 194 (2002)

# Damage function

Displacement damage function (cross section) for various particles as function of their energy (Assumption: damage is proportional to the energy deposited into the displacement interaction)

$D(E)$  in the plot below is divided by 95 mb to be normalized to the damage caused by 1 MeV neutrons:

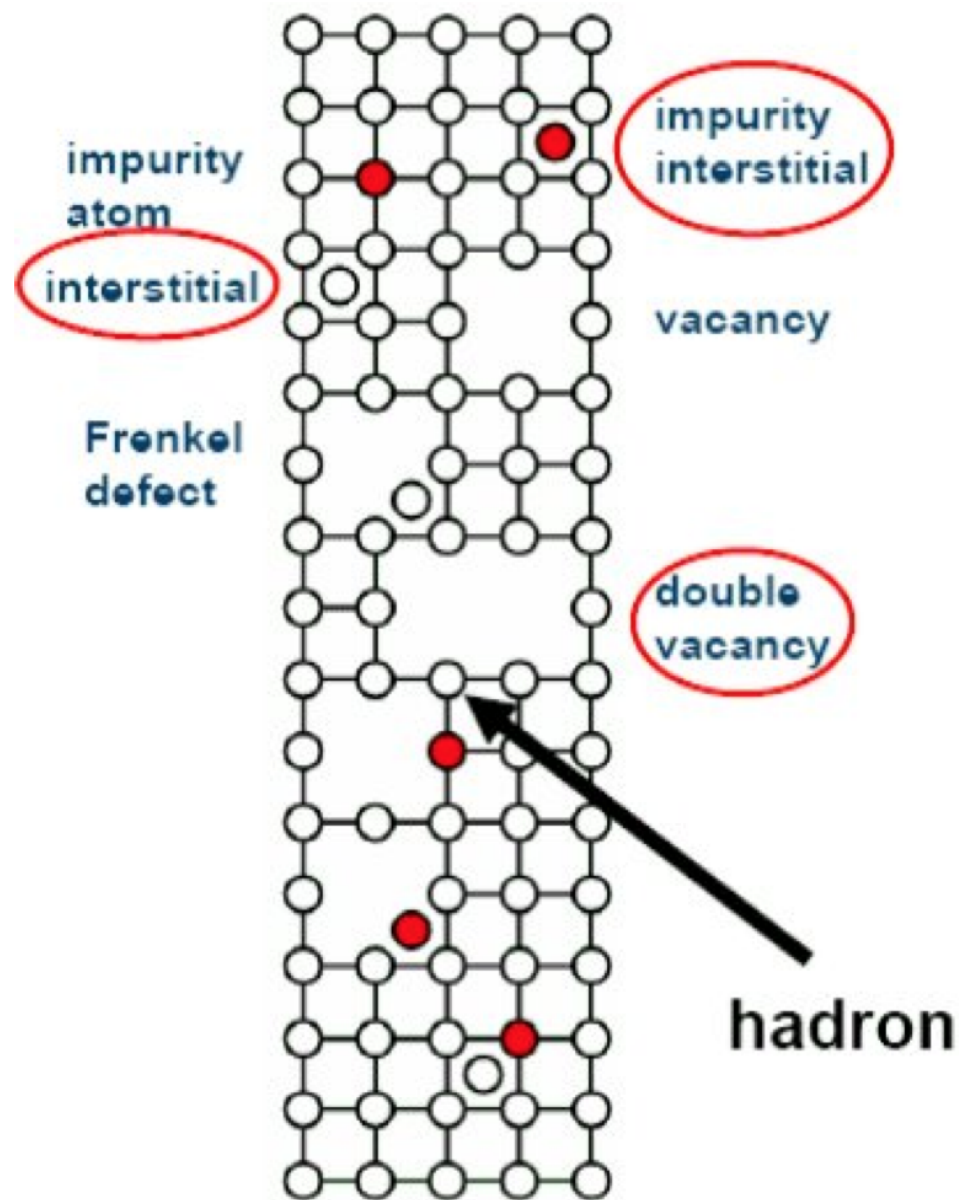


# Annealing and secondary effects

- Interstitials and the position of vacancies are moving inside the crystal lattice and they are not stable defects.
- Some of the dislocated atoms may fall again into a regular lattice position. Both defects disappear! This effect is called annealing.

**Annealing strongly depends on the temperature**

- Some of these primary defects can combine with other defects to create immovable, stable **secondary defects**.

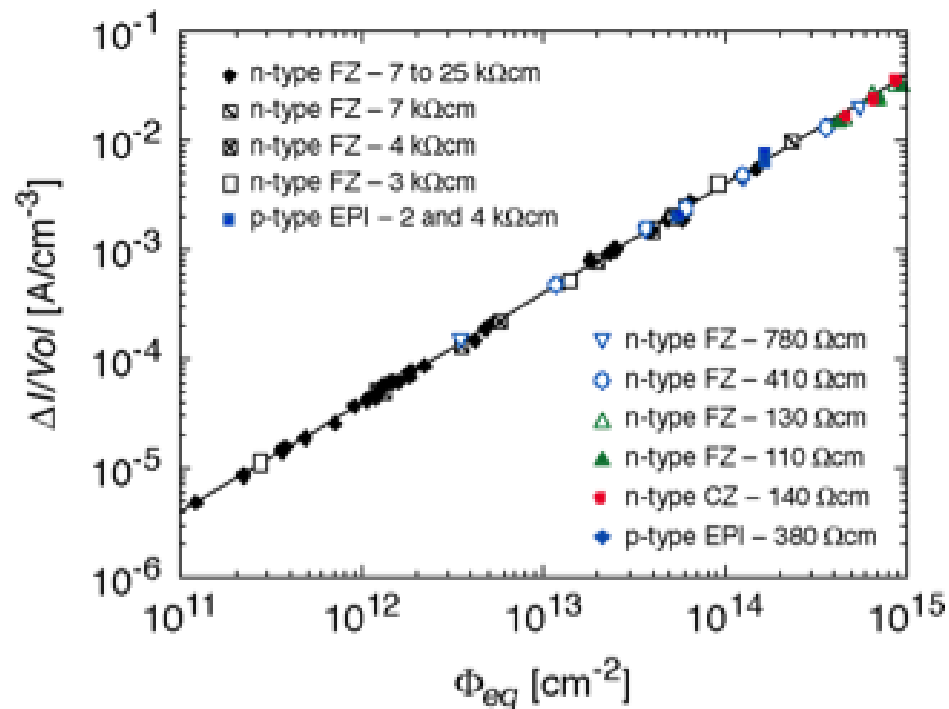


# Leakage current

- Irradiation induced leakage current increases linearly with the integrated flux of radiation:

$$\frac{\Delta I}{Vol} = \alpha \cdot \phi_{eq}$$

- $\alpha$  is called the **current related damage rate**. It is largely independent of the material type.  $\alpha$  depends on temperature, the time between exposure to radiation and measurement (annealing).



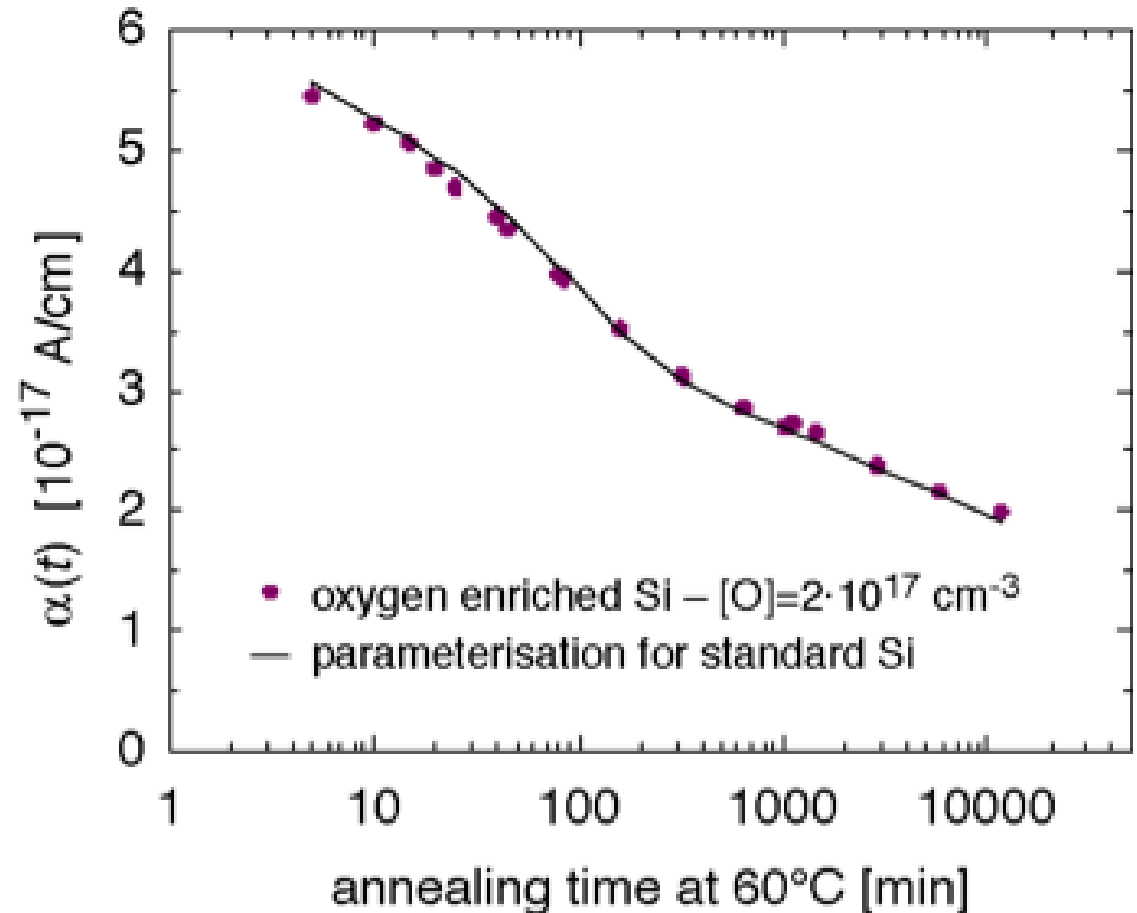
Increase of leakage current as function of irradiation fluence (different materials). Measurement after 80 minute annealing time at 60°C. The linear increase equals to  $\alpha \approx 4 \cdot 10^{-17}$  A/cm.

**In ten years of LHC operation the currents of the innermost layers increase by 3 orders of magnitude!**

# Leakage current: annealing

The damage rate  $\alpha$  is time dependent

The plot shows the development of  $\alpha$  for a detector stored at  $T = 60\text{ }^{\circ}\text{C}$  after irradiation



# Change of effective doping concentration

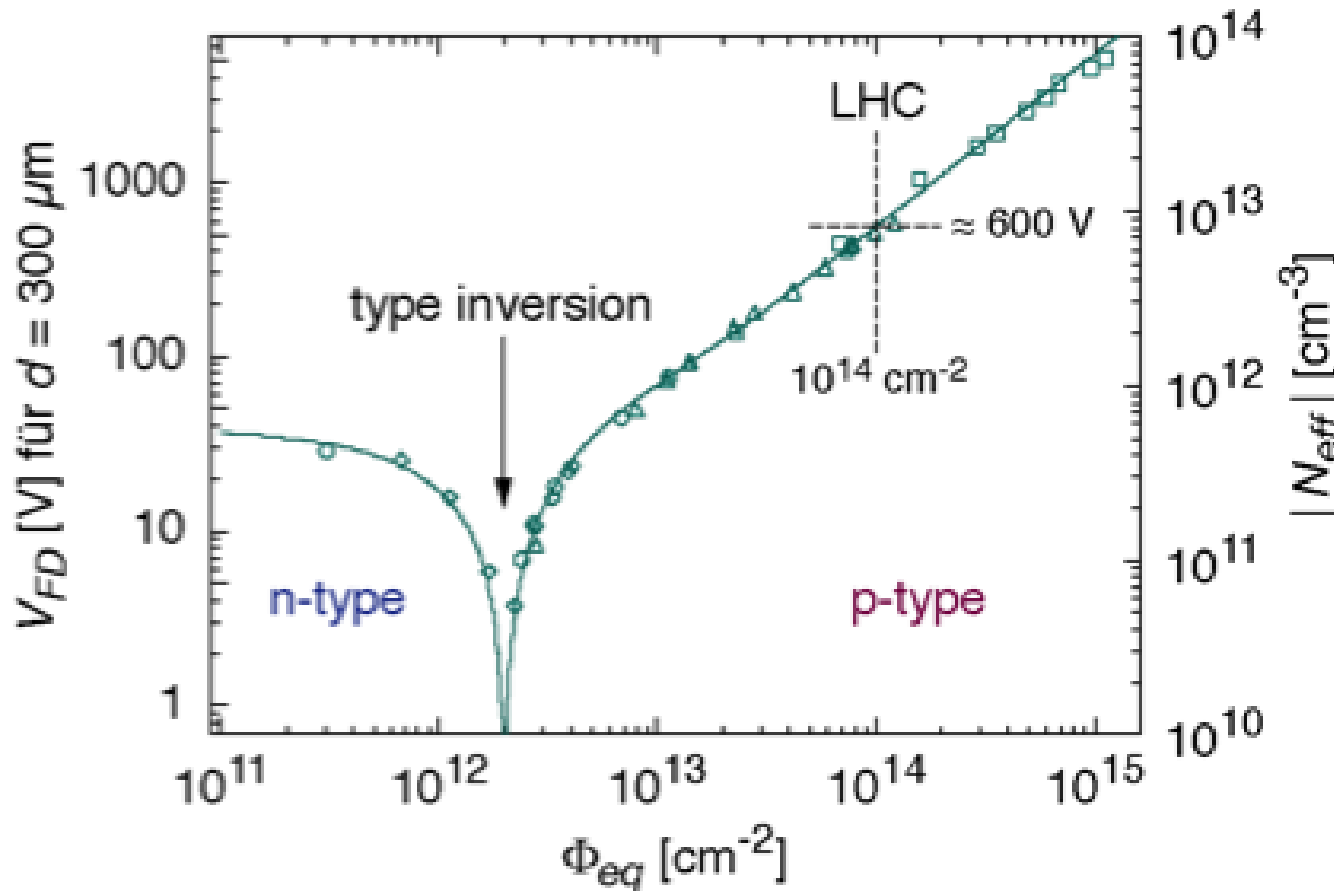
- The voltage needed to fully deplete the detector  $V_{FD}$  is directly related to the effective doping concentration:

$$V_{FD} = \frac{e}{2\epsilon_0\epsilon_r} |N_{eff}| d^2$$

- The irradiation produces mainly acceptor like defects and removes donor type defects. In a n type silicon the effective doping concentration  $N_{eff}$  decreases and after a point called **type inversion** (n type Si becomes p type Si) increases again.
  - The depletion voltage and consequently the minimum operation voltage decreases, and after the inversion point increases again.

# Change of effective doping concentration

Full depletion voltage and effective doping concentration) of an originally n type silicon detector as a function of the fluence  $\Phi_{eq}$

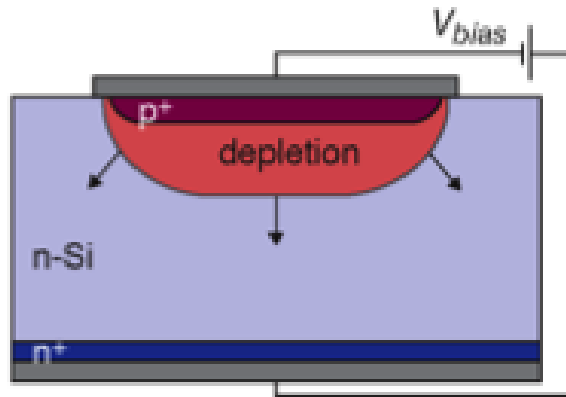


G. Lindström, *Radiation Damage in Silicon Detectors*, Nucl. Instr. Meth. A **512**, 30 (2003)

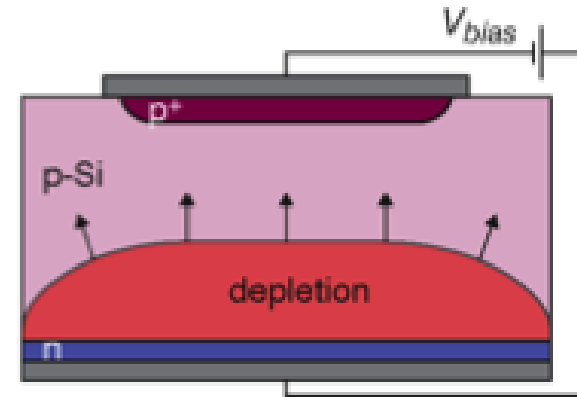
# Operation before and after type inversion

- In n type sensors with p<sup>+</sup> implants the depletion zone grows from the p<sup>+</sup> implants to the backplane n<sup>+</sup> implant. After type inversion the p<sup>+</sup> bulk is now depleted from the backside → **polarity of bias voltage remains the same!**

Unirradiated detector:



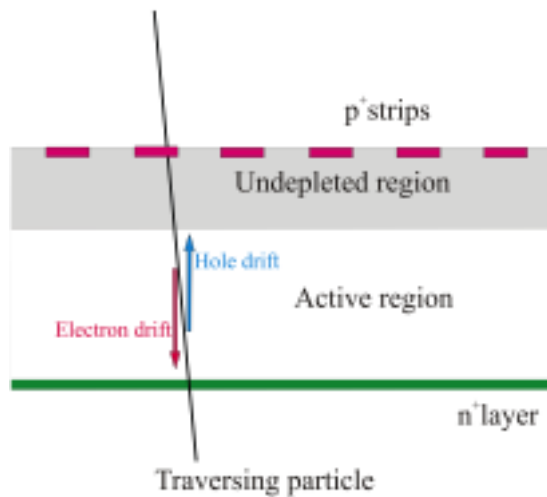
Detector after type inversion:



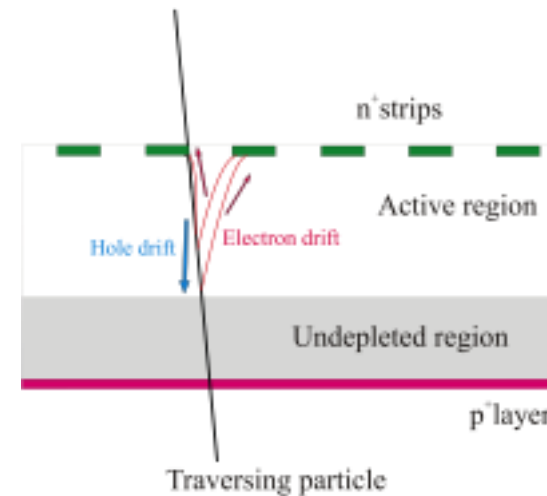
- n-type detectors before type inversion can be operated below full depletion. After type inversion, the depletion zone has to reach the strips. (A possible solution is to use n+p or n+n detectors)

# Operation before and after type inversion

**p<sup>+</sup> n** after high fluences  
n-type silicon is type inverted



**n<sup>+</sup> p** after high fluences  
p-type silicon remains p-type



In case the detector has to be operated under-depleted:

- Charge spread – degraded resolution
- Charge loss – reduced CCE
- Limited loss in CCE
- Less degradation with under-depletion
- Collect electrons (faster than holes)

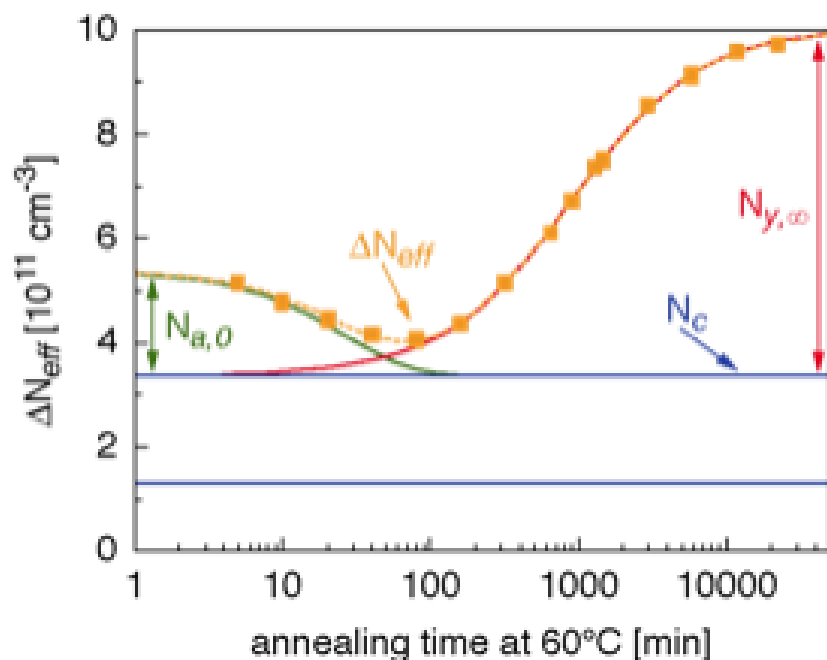
**n<sup>+</sup> p sensors baseline for ATLAS and CMS upgrade detectors.**

Instead of n<sup>+</sup> p also n<sup>+</sup>n devices could be used, but requires double sided processing.

# Annealing and reverse annealing

- The effect of annealing is also seen in the development of the effective doping concentration and the full depletion voltages.
- After some time the annealing process inverts and secondary defects develop and worsen the radiation damage with time **reverse annealing**.

Long time dependence of  $\Delta N_{eff}(t)$  of a silicon detector irradiated with a fluence of  $\Phi_{eq} = 1.4 \cdot 10^{13} \text{ cm}^{-2}$  and storage at a temperature of  $T = 60^\circ\text{C}$ :



- $N_c$  ... Contribution of stable primary defects
- $N_a$  ... Defects disappearing with time – annealing.
- $N_y$  ... Secondary defects developing with time – reverse annealing.

# Operating temperature

- Annealing and reverse annealing are strongly depending on temperature. Both effects increase with temperature.
- Annealing and reverse annealing overlap in time and develop with different time constants.

In an operating experiment (detectors under radiation) the operating temperature of the silicon is a compromise between beneficial annealing and deteriorating reverse annealing.

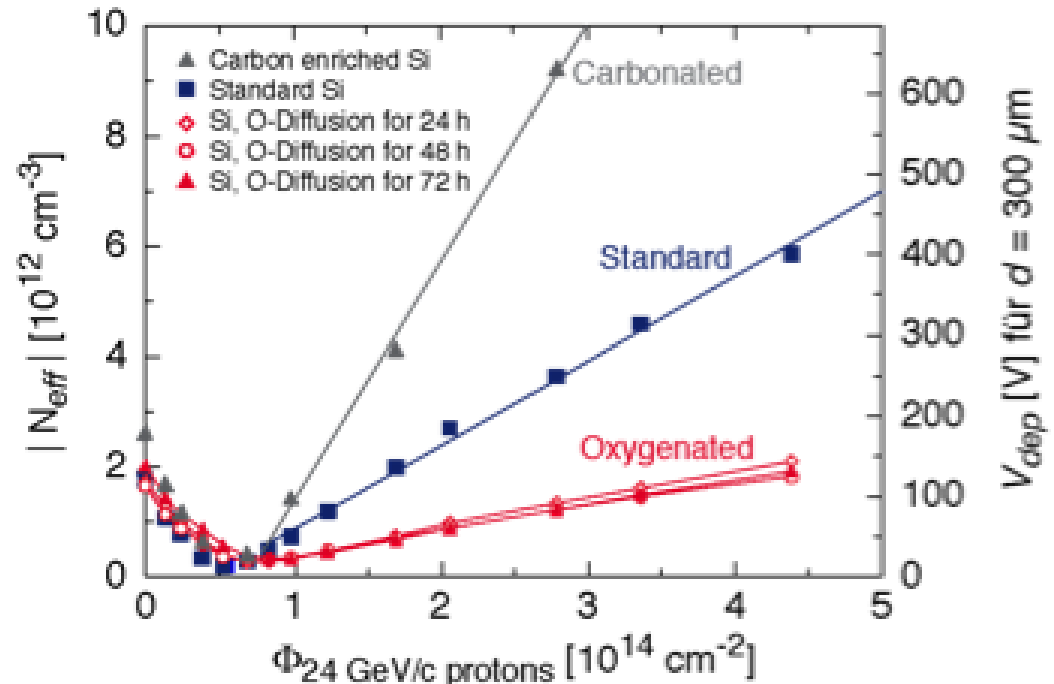
- $N_{eff}$  is relatively stable below a temperature of  $-10^{\circ}\text{C}$ .
- The CMS silicon tracker will be operated at a temperature of  $-10^{\circ}\text{C}$ .
- An irradiated detector has to remain cooled down even in non operating periods.

# Material engineering

- Introduction of impurity atoms, initially electrically neutral, can combine to secondary defects and modify the radiation tolerance of the material.
- Silicon enriched with carbon makes the detector less radiation hard.
- **Oxygen enriched silicon** (e.g. Magnet Czochralski Si) has proven to be more radiation hard with respect to charged hadrons (no effect for neutrons)

Oxygen enriched Si used for pixel detectors in ATLAS and CMS.

Influence of C and O enriched silicon on the full depletion voltage and the effective doping concentration (Irradiation with 24 GeV protons, no annealing):



# Surface defects

- In the amorphous oxide dislocation of atoms is not relevant. However, ionizing radiation creates charges in the oxide.
- Within the band gap of amorphous oxide (8.8 eV compared to 1.12 eV in Si) a large number of deep levels exist which trap charges for a long time.
- The mobility of electrons in  $\text{SiO}_2$  is much larger than the mobility of holes
  - electrons diffuse out of the oxide, holes remain semi permanent fixed
  - the oxide becomes positively charged due to these fixed oxide charges.
- Consequences for the detector:
  - Reduced electrical separation between implants
  - Increase of interstrip capacitance
  - Increase of detector noise
  - Worsening of position resolution
  - Increase of surface leakage current

# Surface defects

---

- The read out electronics is equally based on silicon and  $\text{SiO}_2$  structures.
- Read out electronics is based on surface structures (e.g. MOS process) and hence very vulnerable to changes in the oxide.
- The front end electronics is mounted close to the detector and experiences equal radiation levels.

**Radiation damage is a very critical issue also for the readout electronics!**

# Radiation damage: summary

---

- Silicon detectors are very radiation tolerant
- The defect introduced by radiation change significantly the properties of the detectors
- As long as the bias voltage can follow the development of the full depletion voltage (voltage remains below break down voltage) and the effect of increased leakage current can be controlled (cooling) the detector remains functional.
- Charge trapping, increase of capacitance and leakage current, etc. worsen the performance of the detector gradually.
- The radiation tolerance can be improved by the design of the detector structures, the use of oxygenated silicon, or the development of detectors based on alternative materials (diamond).